ABATEMENT OF SPECTRAL INTERFERENCES IN ELEMENTAL MASS SPECTROMETRY: DESIGN AND CONSTRUCTION OF INDUCTIVELY COUPLED PLASMA ION SOURCES FOR FOURIER TRANSFORM ION CYCLOTRON RESONANCE INSTRUMENTATION

By

KENNETH ERIC MILGRAM

A DISSERTATION PRESENTED TO THE GRADUATE SCHOOL OF THE
UNIVERSITY OF FLORIDA IN PARTIAL FULFILLMENT OF THE
REQUIREMENTS FOR THE DEGREE OF DOCTOR OF PHILOSOPHY

UNIVERSITY OF FLORIDA

1997

Copyright 1997

by

Kenneth Eric Milgram

This dissertation is dedicated to my uncle, James K. May.

ACKNOWLEDGMENTS

A quality dissertation is never the result of a singular effort. Many people have contributed to this dissertation, either through such tangible donations as equipment and funding, or more intangible, but often equally important, ones such as advice and support.

First, I acknowledge my research advisor, Professor John R. Eyler. Despite being chairman of the Chemistry Department, his administrative duties never posed a serious impediment to my graduate education. Additionally, he gave me the freedom to pursue my research goals in an unconstrained manner (often to my own detriment), and I thank him most for this.

Next I thank Dr. Clifford H. Watson for all of the assistance he gave me throughout my graduate career. Whether enduring my continual barrage of technical questions or helping me in the laboratory, Dr. Watson was an indispensable source of knowledge. In addition to Dr. Watson, other members of my research group, either current or past, who deserve acknowledgment for contributing to my research experience are Joe

Nawrocki, David Kage, Maria Wigger, Petia Shipkova, Kevin Goodner, Lisa Lang, Ragulan Ramanathan, Dilrushki Pieris, and Yarjing Yang.

In addition to my research group, there are numerous other individuals within the University of Florida Department of Chemistry who deserve acknowledgments. I thank Professor Samuel Colgate for teaching the glass-blowing/machine shop course that proved invaluable to my graduate research. I also thank him for instilling in me through his rigorous demands of excellence the compulsion to perform any endeavor to the best of my ability.

I owe Mr. Joseph Shalosky a tremendous debt of gratitude. Besides building much of the apparatus used in all stages of this work, he too showed me the value of performing to the best of one's ability. The level of craftsmanship demonstrated in his work is remarkable. Furthermore, his combination of skill, patience, teaching ability, desire to help others, and amiability are unrivaled. I also thank Mr. Mike Herlovich for his machining contributions that made my later experiments such a success. In addition to taking painstaking care with my machining projects and completing them in near record time, Mr. Herlovich was also a very pleasant person to interact with. Other members of the machine shop who deserve acknowledgment are Gary Harding, Todd Prox, Chester Eastman, and Daily Burch.

Another group of important people I wish to acknowledge are often overlooked, but my research experience would have been far less productive without them. They are Ms. Beverly Lisk, Ms. Janet Smith, Ms. Marie Goddard, and Ms. Lisa Reed, all of the fiscal office. Whenever I needed an item immediately, they were always friendly and exceeded the normal expectations of their jobs. I am truly grateful to each of them.

I thank Professor James Winefordner and Dr. Benjamin Smith for allowing me to feel like part of their research group, and for loaning me the bulk of the inductively coupled plasma equipment used for the research presented in this dissertation.

I thank Professor Sam Houk of Iowa State University for his involvement at all key stages of the research presented in this dissertation. His knowledge of sampling ions from plasma and detecting them by mass spectrometry is unrivaled and proved invaluable. Without his direct assistance, this research would not have progressed to its current state.

I thank Dr. David W. Koppenaal and Dr. Charles J. Barinaga, both of Pacific Northwest National Laboratory, for their advice and loan of numerous pieces of equipment that was used throughout the research presented in this dissertation.

I also owe a tremendous debt of gratitude to numerous individuals at the National High Magnetic Field Laboratory. I thank Professor Alan Marshall for the use of his facilities and for purchasing numerous pieces of equipment that were necessary to complete this research. I thank Mr. Forest White for his assistance with some of the work described in Chapter 4 of this dissertation. I also thank Mr. Dan McIntosh for his superb machining contributions that made the work described in Chapter 5 of this dissertation possible.

In addition to the people already mentioned who had a direct impact on my graduate school career, there are a number of others who had a such a profound impact on my life, that they deserve mention here. The first of these people is Professor Donn G. Shilling of the University of Florida Department of Agronomy. The research skills that I acquired under his guidance still continue to serve me today, and they have been more valuable to me than I could have ever realized. Furthermore, Professor Shilling's faith in me as a scientist gave me the confidence and motivation to pursue my dream of attending graduate school. I thank Professor Shilling for all of his expert advice and for giving me the opportunity to experience autonomous research at an early stage in my career.

I also thank Professors Harold Browning and Herbert Nigg at the University of Florida Citrus Research and Education Center. They gave me my first research job, and because of their expert guidance, my interest in research was kindled.

Finally, there is a small group of people who have enriched my life and deserve acknowledgment. I thank my uncle, Mr. James K. May, for his encouragement and assistance throughout my life. His continual support made my educational experience much easier. Two other members of my family who deserve acknowledgment are my mother Norma Johnson, and my brother Anthony Wells. Their unfaltering belief in me gave me the strength I needed to persevere through difficult times.

In addition to my direct family, I also acknowledge the Clevenger family, Brad, Donnie, Marvin and Chad. By treating me as a full member of their family and showing sincere faith in my abilities, I was able to believe in myself. I also wish to thank Dr. Henry Villegas, M.D., for being a good role model, a source of inspiration, and a good friend. His encouragement caused me to evaluate my future critically at an early age, a process which resulted in me pursuing my ambitions. Finally, I thank Erin Huggins. Her patience and understanding towards me while I was writing this dissertation are greatly appreciated.

TABLE OF CONTENTS

ACKNOWLEDGMENTS iv

SYMBOLS xi

ABSTRACT xii

CHAPTERS

1 INTRODUCTION 1

2 FOURIER TRANSFORM ION CYCLOTRON RESONANCE MASS SPECTROMETRY 12
  History 12
  Analytical Advantages of FTICR MS 20
  Disadvantages of FTICR MS 25
  Motions of Ions in a Magnetic Field 28
  Experimental FTICR Sequence 39
  Ion Excitation in FTICR 48
  FTICR Detection 53
  Conclusions 61

3 INITIAL ICP-FTICR SOURCE DESIGN 62
  Inductively Coupled Plasma Mass Spectrometry 62
  First ICP-FTICR Source Design 71

4 INTERMEDIATE SOURCE DESIGNS 80
  Introduction 80
  Experimental Parameters 81
  FTICR Instrumentation 84
  Results and Discussion 91
  Conclusions 101

5 DESIGN AND CONSTRUCTION OF AN OCTOPOLE BASED ICP-FTICR SOURCE 103
  Introduction 103
  Design Considerations 104
  Results and Discussion 109
  Conclusions 117

GLOSSARY 119

REFERENCES 142

BIOGRAPHICAL SKETCH 150

SYMBOLS

$\Delta m_{(x)}$	mass resolution
ν_C	natural ion cyclotron frequency
ν_+	shifted (reduced) ion cyclotron frequency
ν_-	magnetron frequency
ν_T	trapping frequency
ω_C[†]	natural ion cyclotron angular frequency
ω_+	shifted (reduced) ion cyclotron angular frequency
ω_-	magnetron angular frequency
ω_T	trapping angular frequency
$\mathbf{B}$	magnetic field vector
Da	dalton
$m/\Delta m_x$	mass resolving power
m/q	mass-to-charge ratio for an ion (Not equal to m/z)
m/z	see explanation in Glossary
S/N	signal-to-noise
T	tesla
Wb	weber

Note: Conversion of any angular frequency (ω) to its corresponding direct (also known as linear) frequency (ν) is accomplished by division by 2π.

[†] $\omega_c = \omega_+ + \omega_-$

Abstract of Dissertation Presented to the Graduate School
of the University of Florida in Partial Fulfillment of the
Requirements for the Degree of Doctor of Philosophy

ABATEMENT OF SPECTRAL INTERFERENCES IN ELEMENTAL MASS SPECTROMETRY: DESIGN AND CONSTRUCTION OF INDUCTIVELY COUPLED PLASMA ION SOURCES FOR FOURIER TRANSFORM ION CYCLOTRON RESONANCE INSTRUMENTATION

By

Kenneth Eric Milgram

December 1997

Chairman: John R. Eyler
Major Department: Chemistry

Elemental analysis is widely employed in a range of disciplines as disparate as geology and nutrition. Unarguably, the single most versatile elemental analysis technique is that of inductively coupled plasma mass spectrometry (ICP-MS), a technique that offers an unparalleled combination of sensitivity, multi–element capability, and knowledge of isotopic content of a sample.

The most serious hindrance to ICP-MS as a technique is the presence of spectral interferences, species which occur in ICP-MS when a background ion has a mass–to–charge ratio that is only nominally different from that of an

analyte ion. With respect to the ability to distinguish spectral interferences from analytes, conventional ICP-MS instrumentation is somewhat limited.

This dissertation reports the design, construction and performance of four novel ICP-MS instruments. Whereas traditional ICP-MS instrumentation consisted of quadrupole or sector–based devices, the instruments discussed in this dissertation incorporated Fourier transform ion cyclotron resonance (FTICR) mass spectrometers because of their ability to produce spectra with resolving power that is unrivaled.

Because of the large difference in operating pressures between an inductively coupled plasma (ICP), which operates at atmospheric pressure, and an FTICR instrument, which operates at 10^{-8} torr or lower, an interface incorporating both enhanced differential pumping and ion transmission simultaneously had to be designed and constructed.

Data collected from initial source designs were used to construct the final interface, a device that incorporated an rf–only octopole for high ion transport efficiency. The octopole was constructed by us, and the electronics to operate it were assembled from items that are readily available commercially. The operation of the interface is discussed in detail, along with spectra acquired with it that demonstrate mass resolving power that is a factor of two greater than any previously reported by the ICP–MS technique.

CHAPTER 1
INTRODUCTION

Inductively coupled plasma mass spectrometry[1,2,3,4] (ICP-MS) is a powerful analytical technique for trace elemental analysis. It has been applied routinely to problems in disciplines as disparate as geology and nutrition. Some advantages of ICP-MS include low detection limits (subpart–per–trillion), nearly simultaneous multi–element analysis capability, inherent isotopic information, short analysis times (minutes), and easy spectral interpretation (compared to optical methods). An ICP is an excellent source for generating atomic ions because most elements are ionized efficiently in the plasma.[5] Furthermore, over 90% of the ions formed are singly charged,[6] a feature which simplifies mass spectrometric interpretation.

Despite these desirable characteristics, ICP–MS, like all analytical techniques, has its limitations. Spectral interferences (*i.e.*, those which cause an erroneously large signal to be measured for a particular analyte) are the biggest hindrance to ICP–MS. Although they may have other origins, spectral interferences usually occur in ICP–MS when ions (*e.g.*, background ions or other analyte ions) possess the same nominal m/z value as a given analyte ion. These interfering ions can be divided into two major categories—polyatomic and isobaric. Despite the harsh, high-energy and high-temperature environment of the plasma, some polyatomic ions either survive or are formed within the plasma. Polyatomic ions can also be formed when the high temperature plasma interacts with the much cooler sampling interface.

Isobaric ion interferences (*e.g.* $^{40}Ar^+/^{40}Ca^+$) occur when background elements are present in the sample with masses that are only nominally different from those of the elements being determined. Although most elemental ions are singly charged within the plasma, doubly charged atomic ions can also pose a problem when their m/z is only nominally different from an analyte of interest.

A considerable amount of ICP-MS literature has been dedicated to isobaric and polyatomic ion interferences. For example, Evans and Giglio published a lengthy review of the origins and categories (spectral and nonspectral) of ICP-MS interferences along with concise methods for alleviating them in a large variety of sample matrices.[7] Sah published a similar work with a focus on biological and environmental samples.[8] Reed *et al.* catalogued polyatomic ion interferences for elements from Li to Ge;[9] however, this study, like most studies to date, simply ignored interferences that required mass resolving power ($m/\Delta m_{10\%V}$, *see mass resolving power* in the **Glossary**) greater than 10,000, the current practical upper limit for conventional ICP-MS instrumentation.

Many strategies for remedying polyatomic ion interferences involve removal of the interfering species prior to detection by the mass spectrometer. Tanner reported the suppression of Ar^+ and ArO^+ signals by adjusting incident power and aerosol gas flow rates to favor a "cool" plasma.[10] Numerous workers have reported a reduction in polyatomic species by thorough solvent removal.[11,12] Clemons *et al.* reported a reduction in the signal due to metal oxides with the use of a heated, graphite torch injector in conjunction with desolvation.[13] Chemical separations have also been employed to reduce both polyatomic and isobaric ion interferences in ICP-MS.[14,15] Mathematical corrections for spectral interferences[16,17] have been applied to ICP-MS, but these techniques usually require some prior knowledge of the sample. Mixed gas plasmas[18,19] (*e.g.*, argon-xenon) have been shown to alleviate polyatomic ion interferences in some cases. Finally, gas phase reactions in ion traps and multipoles have recently been used to demonstrate dramatic reductions or in some cases, complete elimination altogether, of polyatomic and isobaric ion interferences.[20,21,22,23,24]

The aforementioned methods are deficient in that they tend to address only a narrow set of interferences. The need for ICP-MS methods that are capable of resolving all types of spectral interferences without prior knowledge of sample constituents is evident. One alluring alternative is an ICP-MS instrument equipped with a high resolution mass analyzer. The most common high resolution mass analyzer in ICP-MS is a double focusing magnetic/electric sector device.[25] Commercial availability from three different manufacturers (Finnigan, Jeol, and MicroMass, formerly Fisons/VG) indicates that these instruments have found a niche. When operated in a low resolution mode (e.g., $m/\Delta m_{10\%v} < 500$), these instruments have very high transmission efficiencies, which when combined with their low background noise counts, result in superior detection limits. The practical upper limit of mass resolving power ($m/\Delta m_{10\%V}$) for most high resolution sector instrument analyses is about 10,000; however, Morita *et al.* were able to resolve $^{76}Ge^+/^{76}Se^+$ ($m/\Delta m_\delta = 34,700$, *see theoretical mass resolving power* in the **Glossary**) and $^{150}Sm^+/^{150}Nd^+$ ($m/\Delta m_\delta = 41,500$) with an extreme sacrifice in sensitivity, resulting in detection limits of nominally 1 mg/L.[26] Although these mass resolving powers are sufficient to resolve many interferences that cannot be separated with quadrupole based instrumentation, many analyses remain that simultaneously require greater mass resolving power and sensitivity. The determination of trace levels of radionuclides (e.g. $^{63}Ni^+$ and $^{238}Pu^+$) amidst large, natural isotopic backgrounds is one important example where high to ultra-high mass resolving power is required for analysis by ICP-MS. Table 1-1 lists just a few examples of analyte ions and potential interferences that require greater than 10,000 mass resolving power for separation.

Table 1-1: Some Atomic Ions, Potential Interferences, and Mass Resolving Power Required to Separate the Pair

Atomic Ion[a]	**Natural Abundance**[b]	**Potential Interference**[c]	**$m/\Delta m_\delta$**
$^{40}Ca^+$	99.6%	$^{40}Ar^+$	193,000
$^{63}Cu^+$	69.2%	$^{62}Ni^1H^+$	18,300
$^{74}Ge^+$	36.5%	$^{74}Se^+$	57,000
$^{106}Pd^+$	27.3%	$^{106}Cd^+$	35,500
$^{127}I^+$	100%	$^{110}Cd^{16}O^1H^+$	100,000
$^{133}Cs^+$	100%	$^{116}Cd^{16}O^1H^+$	64,400
$^{139}La^+$	99.9%	$^{122}Sn^{16}O^1H^+$	825,300
$^{141}Pr^+$	100%	$^{124}Sn^{16}O^1H^+$	385,300
$^{187}Re^+$	62.6%	$^{187}Os^+$	62,300,000
$^{63}Ni^+$	N/A	$^{63}Cu^+$	21,300
$^{99}Tc^+$	N/A	$^{99}Ru^+$	183,000
$^{129}I^+$	N/A	$^{129}Xe^+$	678,000
$^{238}Pu^+$	N/A	$^{238}U^+$	319,000

[a] The listed isotope is the most abundant for the indicated element.

[b] Natural abundance for the isotope indicated in the Atomic Ion column. Radioactive isotopes are indicated by "N/A" (not applicable) for the natural abundance.

[c] Each isotope comprising the listed interference has a natural abundance greater than 0.01%.

Current high-resolution sector based ICP-MS instruments have a major drawback: an intrinsic tradeoff between sensitivity and resolving power. To increase the resolving power of a sector based instrument, the slits which are responsible for constraining the detected m/z range are narrowed, resulting in decreased ion transmission efficiency (see Figure 1-1). Compared to a 100% normalized signal at a mass resolving power of 500, the signal observed when $m/\Delta m$ is increased to 5000 will be only 1/10 of its original value. When $m/\Delta m$ is increased to about 8,000, the signal will have decreased to about 1-2% of its value at $m/\Delta m=500$.[27]

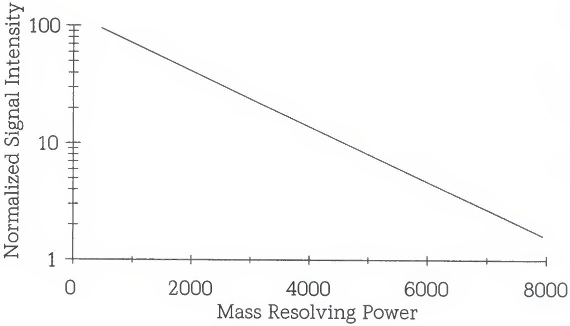

Figure 1-1
Typical relationship between ion transmission efficiency and resolving power observed with double focusing sector instruments. (Adapted from reference 27)

Quadrupole based ICP-MS instruments have also demonstrated potential for producing high resolution spectra. Ying and Douglas separated $^{56}Fe^+$ from $^{40}Ar^{16}O^+$ ($m/\Delta m_\delta \approx 2{,}500$) by operating a quadrupole mass filter in the second stability region.[28] Analytical sensitivities were obtained that were comparable to those of a sector based instrument operating at the same mass resolving power (*e.g.*, 10^6 ions/s per mg/L of element in solution). Such performance represents the upper limit for quadrupole based instrumentation because operation of a quadrupole within alternate stability regions requires very high rf voltages. Additionally, these regions are not well characterized, and mass discrimination becomes much more pronounced. Lastly, the usable m/z range is reduced.

The benefits of ultra-high resolution elemental mass spectrometry have already been demonstrated by the Eyler group via incorporation of a glow discharge source with a Fourier transform ion cyclotron resonance (FTICR) mass spectrometer.[29,30,31,32,33] Glow discharge[34,35] mass spectrometry (GD-MS) is an elemental analysis technique that is used primarily for the analysis of solid, metallic samples, although it has also been applied to both liquid and nonconducting samples. FTICR MS[36,37] is a mass spectrometric technique that possesses the following features: ultra-high mass resolving power ($m/\Delta m_{10\%V} > 10^6$), excellent mass accuracy (better than 1 part-per-million), excellent sensitivity, simultaneous detection of all ions over a wide mass range (multiplex advantage), the ability to remove unwanted ions selectively from the analyzer cell, and the ability to perform multiple stages of tandem MS (MS^n capability).

An impressive demonstration of the ultra-high mass resolving power capability of FTICR was reported by Wanczek's group recently. They obtained resolving power in excess of 2×10^8 ($m/\Delta m_{50\%}$) for an isotope of Xe.[38] Such resolving power is sufficient to eliminate any spectral interference of chemical origin encountered in ICP-MS (probably in any type of mass spectrometry).

The multiplex advantage of FTICR allows for a good duty cycle; for example, a high resolution spectrum ($5{,}000 < m/\Delta m_{10\%V} < 30{,}000$) covering a wide mass range (10 – 4,000 m/z) can be obtained in a matter of seconds (typically, 1 second). Ultra-high mass resolution spectra ($m/\Delta m_{10\%V} > 10^6$) can be obtained in times ranging from several seconds to several minutes, depending on the m/z value of the ion of interest and the applied magnetic field strength. In applications where it is necessary to determine many elements simultaneously, the duty cycle of an FTICR instrument is at least as good as that for a quadrupole based ICP-MS instrument. Under practical operating conditions, the dwell time (amount of time spent per m/z unit) for quadrupole instruments is about 1 s. If 30 masses are to be determined, the quadrupole instrument will require 30 seconds per spectrum. By contrast, the FTICR instrument requires only about 1 second to detect the same (or an even greater) number of masses. The multiplex advantage of FTICR was exploited recently by Eyler's group to analyze 8,000 compounds simultaneously that were present in a combinatorial library, each in low picomole amounts.[39] The average analysis time for these combinatorial libraries was about one second, and individual isotopes were resolved.

With regard to sensitivity, image current detection—the detection method used in FTICR—is less sensitive by a factor of approximately 100 than electron multiplier detection. Even so, FTICR MS's ability to remeasure a single ion population repeatedly can partially compensate for this reduced sensitivity, especially in applications where sample ions are not generated continuously.[40,41]

Despite the reduced sensitivity of image current detection, some recent publications document the impressive detection limits that have been obtained with FTICR MS. Valaskovic *et al.* sequenced attomole levels of carbonic anhydrase using ESI-FTICR with flow rates in the nanoliter per minute range.[42] Full spectra were obtained with 60,000 mass resolving power and mass errors of less than 1 Da for proteins in the range 8–29 kDa. Using a MALDI source, Solouki *et al.* obtained low attomole detection limits for numerous singly and multiply charged biomolecules with a 3.0 T system.[43]

Bruce *et al.* were able to detect a single molecule of bovine serum albumin with a 7.0 T ESI-FTICR system.[44]

In cases where even FTICR is unable to resolve polyatomic ion interferences, the MS^n capability could be useful. Fragmentation of the interferences would permit their simultaneous identification and removal. The extra stage of MS would increase analysis time somewhat; therefore, MS^n might only be used when a particular polyatomic interference could not be resolved.

Finally, an FTICR MS instrument (unlike sector instrumentation) does not suffer from a trade off between ion transmission efficiency and resolving power. For a given set of data processing conditions, an *increase* in mass resolving power will usually be accompanied by an *increase* in S/N.

The work presented in this dissertation chronicles the development of a new analytical technique which was conceived and developed at the University of Florida, namely "inductively coupled plasma Fourier transform ion cyclotron resonance mass spectrometry" (ICP-FTICR MS). Fundamentals of FTICR MS are discussed in Chapter 2. In the beginning of Chapter 3, some fundamentals of ICP-MS are discussed; the remainder of the chapter discusses our initial design efforts. In Chapter 4, early ICP-FTICR ion source designs and the results obtained with them are discussed. Chapter 5 is devoted to the discussion of a vastly improved ICP-FTICR ion source. A unique feature of this source was the incorporation of an octopole ion guide to improve ion transport efficiency. This chapter also unifies all of the work discussed in the preceding chapters and concludes with a discussion of future work.

CHAPTER 2
FOURIER TRANSFORM ION CYCLOTRON RESONANCE MASS SPECTROMETRY

History

The application of the principle of ion cyclotron resonance (ICR) for analytical purposes can be traced back to the classic experiments of E. O. Lawrence and M.S. Livingston in the 1930s.[45] By application of an electric field oscillating at the correct frequency, charged atomic and subatomic particles, which were constrained to a circular path by magnetic fields, were accelerated to very high kinetic energies for the study of nuclear physics. Lawrence was awarded the 1939 Nobel Prize in physics for his development of the ion cyclotron.

The principle of ion cyclotron resonance was not used for mass analysis until the development of the Omegatron by a group at the National Bureau of Standards in 1949.[46] With the Omegatron, detection was accomplished by continually measuring the current generated as ions resonantly absorbed rf energy and increased their orbital radius enough to strike a set of detection electrodes. Although the instrument was used as a mass measurement standard, its primary use was for residual gas analysis because it could be used only over a narrow mass range.

In the early 1960s, the first ICR mass spectrometer that utilized "resonant" detection was developed by Wobschall *et al.* at Cornell.[47] Although this instrument was severely limited with respect to scan speed (approximately 30 minutes per spectrum) and mass resolving power (unit mass), it was invaluable to those interested in gas phase ion-molecule chemistry.[48] An early application of ICR was Brauman and Blair's determination that the gas phase acidity of toluene was greater than that of water,[49] a remarkable result considering that water is about 10^{20} times more acidic than toluene in the liquid phase. Wobschall's ICR became commercially available as Llewellyn's "ion cyclotron resonance" (ICR) mass spectrometer.[50]

By 1970, the Fourier transform (FT) mode of operation had been applied to infrared (FTIR)[51] spectrophotometry and nuclear magnetic resonance spectroscopy (FTNMR). The multiplex advantage, the major benefit of the FT mode of operation, resulted in a tremendous time savings compared to the single channel detection method which was originally employed in these techniques. With the FT mode of operation, spectra could be acquired in much less time with S/N and mass resolving power as good as that obtained with the single channel method. Additionally, acquisition for longer times resulted in spectra with mass resolving power and S/N that was orders of magnitude greater than that which could be obtained in the conventional mode of operation. Because of its advantages, the FT mode of operation quickly superseded the single channel mode for these techniques.

Ion cyclotron resonance mass spectrometry would not experience the benefits from the FT mode of operation until 1974 because of a lack of several key technologies. For one, there was no good method of storing a range of ions of widely varying m/z simultaneously for the length of time necessary to perform a mass measurement by the FT method. Furthermore, a method was needed that would allow resonant excitation of all ions over a broad m/z range (*i.e.,* broadband). Also needed was a method of detecting all ions simultaneously. Finally, to gain the benefits of the FT mode of operation, a fast digitizer with sufficient memory and bit resolution would be required, and such devices were only just becoming available in the early 1970s.

The problem of ion storage was solved in 1971 with the development of the trapped ion cells by McIver.[52] As for exciting a wide mass range of ions simultaneously, Melvin Comisarow solved the problem by thinking about excitation in conventional ICR, where a slow frequency sweep with an amplitude of a few mV was used to excite one ion at a time over a long period.[53] By analogy, Comisarow reasoned that a rapid frequency sweep of a few tens of volts amplitude should also be capable of exciting a wide mass range of ions, but in a much shorter time.

The detector in use at the time for ICR was a marginal oscillator. This device was capable of detecting only a single frequency at time, and it could not be tuned over a wide frequency range quickly. Instead of measuring power absorption, Marshall and Comisarow decided to measure the image current induced in a set of nearby electrodes by an ensemble of ions undergoing cyclotron motion. With no suitable detector available commercially, Comisarow constructed his own broadband amplifier capable of measuring simultaneously the minuscule currents produced from a range of ions with very different m/z values. In late 1973, with the initial technological constraints removed, Marshall and Comisarow demonstrated the advantages of the FT mode of operation of ICR mass spectrometry.[54]

Once the time domain spectrum had been acquired with their first FTICR instrument, the first 256 data points (not 256 k!) were saved to magnetic tape, then transferred to a computer which performed the fast Fourier transform (FFT) based on the Tukey-Cooley algorithm[55] to obtain the frequency domain spectrum. Incidently, the Tukey-Cooley publication of the FFT algorithm has become the most highly cited paper in all of mathematics.[56]

Despite data acquisition hardware that would be considered unsuitable by today's standards, Marshall and Comisarow's FTICR instrument was capable of obtaining spectra in about 25 ms. The obtained values for S/N and mass resolving power ($m/\Delta m$) were comparable to those of the single channel mode of detection, a remarkable fact considering the tremendous time savings of the FT mode of operation (30 minutes vs. 25 ms). Some of the parameters from that first instrument are included in Table 2-1.

Table 2-1

Experimental Parameters from First FTICR Experiment	
Magnetic Field Strength[a]	0.32 T
Digitization Rate:	10 kHz (5 kHz bandwidth)
Digitizer Memory:	1024 samples
Digitizer Bit Size:	8 bit (dynamic range = 256)
Excitation mode	single frequency
Excitation frequency	307.126 kHz
Detection mode	heterodyne
Band Pass	1.5 kHz low pass

[a] See **Notes** for *magnetic field strength* and *magnetic flux density* in the **Glossary**

The first commercially available FTICR mass spectrometer was introduced by Nicolet instruments[†] (Madison, Wisconsin) seven years after

---

[†] Now owned by Finnigan and known as the Finnigan FT/MS group

Comisarow and Marshall's first demonstration of FTICR. The Nicolet instrument was equipped with a superconducting magnet that provided high mass-resolving power ($m/\Delta m_{50\%H} > 100{,}000$). Two other manufacturers of FTICR instrumentation emerged during the 1980s, Spectrospin AG[††] (Zurich, Switzerland) and IonSpec Corporation (Irvine, CA).

To a limited few who were primarily interested in ion-molecule reactions, FTICR was unrivaled as a technique. However, to the majority of the analytical community, FTICR, despite its numerous analytical advantages, was considered to be an esoteric technique that was of little value in solving the "real-world" kinds of problems normally handled by other mass spectrometric techniques. As a result, the number of FTICR instruments sold paled in comparison to that of other types of mass spectrometers. One of FTICR's biggest advantages, namely ultra-high mass resolving power, was regarded by many as superfluous. One of its other advantages, namely the ability to trap ions, was also a feature of the quadrupole ion trap (QIT), a mass spectrometer introduced by Finnigan in the early 1980s for almost 1/10 the cost an FTICR instrument. Additionally, the QIT offered much greater sensitivity, and being similar in size to a gas chromatograph, it could be placed on a benchtop. By contrast, an FTICR instrument was perceived by many to be lacking in sensitivity, and as far as space was concerned, an FTICR instrument with a superconducting magnet required a small room. Furthermore, computing restraints prevented FTICR from reaching its full potential. Unlike other types of mass spectrometry where the mass spectrum is detected directly, the spectrum acquired with an FTICR instrument (*i.e.*, time domain) must be further processed by the computationally intensive fast Fourier transform (FFT) routine to yield the resulting mass spectrum. Such a detection scheme combined with a slow computer precludes observation of a mass spectrum in "real-time," a disadvantage that makes operation of the instrument somewhat more difficult. Dedicated FT array processors became available in the late 1980s that could perform an FFT very quickly, but they were expensive (e.g. greater than $10,000). Furthermore, because of limitations in digitizer memory, FTICR instruments were not capable of obtaining ultra-high resolution spectra over wide mass ranges.

[††] Now known as Bruker Daltonics (Billerica, MA)

Although demand for FTICR instrumentation was limited, an ever increasing number of instruments were sold. Throughout the 1980s significant improvements were made to the technique such as the introduction of external source instruments and the development of SWIFT excitation (see *Ion Excitation in FTICR* later in this chapter). Improvements in computing such as menu-driven interfaces also benefitted FTICR. Because of limitations imposed by the early computer interfaces, users of FTICR instruments had to specify instrumental parameters in non-intuitive terms such as bandwidth, excitation amplitudes, cut-off frequencies, *etc*. Such a characteristic made the technique appear dauntingly difficult compared to other types of mass spectrometry. By taking advantage of the improved user interfaces, data acquisition software was written that allowed users to specify instrumental parameters in familiar, intuitive terms such as mass range to be excited and detected, masses to be ejected, excitation energy, and so forth.

Another factor that originally limited FTICR's analytical utility was the requirement for ultra-high vacuum (*i.e.*, pressures $\leq 10^{-8}$ torr) in order to reap the benefits of the technique. Such a stringent requirement limited the types of sources, and hence the samples, that could be analyzed by FTICR. The introduction of external source FTICR instruments by IonSpec Corp. (Irvine, CA) and by Nicolet (Madison, WI) in 1983 permitted atmospheric pressure ionization sources to be used with an FTICR instrument.

Unarguably, electrospray ionization[57,58] (ESI) did more to increase awareness and interest in FTICR than any other single factor. The ultra-high mass resolving power of FTICR allowed individual isotopes to be observed in mass spectra, even for very large molecules (*e.g.*, bovine serum albumin, FM≈60 kDa). Knowledge of the isotopic spacing allows for determination of the number of charges attached to an ion, which in turn can be used to determine the ion's mass (as opposed to m/z). Additionally, the high precision mass accuracy allowed minor modifications to be observed (e.g., addition of adducts or substitution of residues) directly in the gas phase. Finally, in addition to determination of higher order protein structure, the MS^n capability of the technique permitted direct sequencing of biomolecules in the gas phase.[59,60,61]

After a slow period of commercial growth initially, FTICR has begun to proliferate as evidenced by a surge of recent purchases. Companies such as Dupont, Abbott Laboratories, Smith-Kline Beecham, Merck, and Bristol-Myers Squibb, to name a few, have all purchased FTICR instrumentation recently. Given the high cost of FTICR instrumentation and corporate reluctance to invest in unproven technologies, these recent purchases serve to illustrate that FTICR has evolved to fulfill a unique analytical role.

Analytical Advantages of FTICR MS

There are numerous references that describe FTICR in detail,[62,63,64,65] therefore only a brief discussion of the techniques most relevant advantages will be given here.

Ultra-High Mass Resolving Power and High Mass-Accuracy

The most notable attribute of FTICR is probably its ability to produce spectra with ultra-high mass resolving power and high mass-accuracy.[66,67] As was mentioned in Chapter 1, spectra with resolving power in excess of 2×10^8

($m/\Delta m_{50\%}$) have been obtained with FTICR instrumentation. Spectra with mass errors of less than 1 part in 10^5 can be measured routinely, and even better performance can be obtained under more stringent conditions.[68,69] The determination of charge state from the isotopic spacing[70] and its advantages were already mentioned in the previous section. The high mass resolving power is also useful for elimination of spectral interferences that are chemical in origin. Such interferences can appear with any type of sample or ionization source, but they are particularly problematic in elemental analysis. These types of interferences are classified and discussed at length in Chapter 3.

Spectra in which the masses of the species are known with a high degree of precision have obvious advantages compared to low resolution spectra. High precision masses allow for a more unambiguous assignment of species. Additionally, they can be used with simple computer programs to narrow greatly a list of possibilities based on molecular formula.

As mentioned in Chapter 1, there is no severe tradeoff between mass resolving power and sensitivity with the FTICR technique; thus, FTICR is one of the few analytical techniques where a large increase in sensitivity or resolving power does not necessarily result in a decrease of the other. The reason FTICR does not suffer from this weakness can be understood by comparing the basis of identification in different analytical methods

With sector instrumentation, ions are dispersed on the basis of kinetic energy. Identification is made based on the degree to which the ion is dispersed. The selected m/z range is then passed through a slit to be detected. To increase mass resolving power with this technique, the slits are set admit a smaller and smaller range of ions with a given m/z. In this process, analyte signal is inevitably lost. By contrast, no dispersal device is necessary in FTICR because all ions are detected simultaneously.

Multiplex Advantage

Because all ions over the entire usable m/z range can be detected at once, the duty cycle of an FTICR instrument is very good. The average time required for acquisition of a broadband spectrum is approximately 1 second. Depending upon the m/z range to be observed and the applied magnetic field strength, the mass resolving power ($m/\Delta m_{50\%}$) of a broadband spectrum can easily exceed 30,000. The time required to obtain spectra with ultra-high resolving power can be significantly longer, anywhere from 10 seconds up to about 3 minutes, depending upon the m/z range and the applied magnetic field strength.

Trapping and Multiple Stages of Tandem MS (MS^n) Capability

The FTICR method is certainly one of the most versatile techniques available[71] for the gas phase study of ion-molecule reaction pathways,[72,73,74] kinetics,[75] equilibria,[76] and energetics.[77,78] Once ions are stored within the trap, they can be selectively "heated" to induce reactions. Additionally, unwanted ions can be ejected from the trap, a feature that facilitates understanding of a chemical system with many components.

With the MS^n capability, structural elucidation can be greatly simplified. For example, in Figure 2-1, **ABCD** represents a molecular ion. Its m/z can be obtained in the first stage of MS. Next, it can be induced to fragment by increasing its kinetic energy via application of rf energy at a frequency equal to its cyclotron frequency (*i.e.*, resonant) so that it will undergo high-energy collisions with a collision gas. Depending upon the properties of **ABCD**, a number of different combinations of fragments could be obtained, each with the possibility of being neutral or charged. For the sake of this example, it is assumed that **ABCD** will break into two fragments, and that only one fragment will be charged in each stage of MS. Ion **AB** could be mass selected and induced to fragment in a manner analogous to its "parent," **ABCD**. In the third stage of MS, ion **A** would be observed. By calculating the mass-loss during each stage of MS, the identity of **ABCD** could be readily determined. Although this example may seem somewhat contrived, the MS^n capability of FTICR has been used successfully to sequence biomolecules such as oligonucleotides,[79] proteins,[80] and peptides.[81]

Another characteristic of FTICR that can be beneficial to MS^n analyses is nondestructive detection. Because the detected FTICR signal is induced by the ions (*i.e.*, image current detection), the ions are not consumed during the detection process and are available for subsequent experiments.

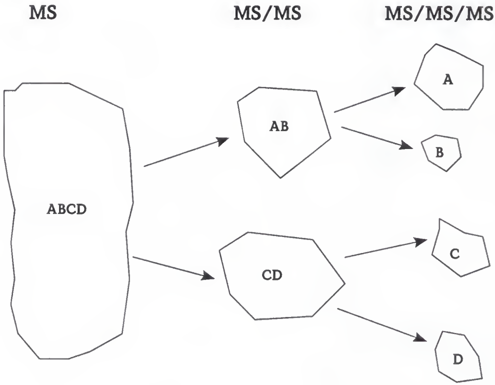

Figure 2-1
Symbolic representation of an MS^n experiment.

Two–Dimensional Capability

Two–dimensional FTICR has also been demonstrated as a means for gathering and analyzing kinetics data for all species in complex, interdependent chemical system simultaneously.[82] For those familiar with FTNMR, 2–D FTICR is directly analogous to 2–D exchange NMR spectroscopy (*i.e.*, NOESY).[83]

Agreement Between Theory and Experiment

Finally, another important advantage of FTICR is the excellent agreement between theoretical predictions and experimental observations, a feature which stems from the fact that the measured FTICR signal is linear with respect to the excitation amplitude.[84] Theory has been used successfully to predict the effect of every major parameter (*e.g.*, magnetic field strength,[85] pressure/acquisition time,[86] number of ions,[87] and noise[88]) on the mass resolving power and S/N of an FTICR signal. Good agreement between theory and experiment allows for more efficient formulation of strategies to remedy inherent weaknesses or limitations in the technique.

Disadvantages of FTICR MS

Surely, the factor which has limited the widespread use of FTICR is the cost of the instrument. A typical external source system retails anywhere from between $500 thousand and $1 million US dollars. Of this amount, the magnet is the single most expensive component. The original FTICR instruments were equipped with electromagnets or permanent magnets, but superconducting magnets offer the most stable and highest magnetic fields, both which are critical factors in terms of instrumental performance. Another disadvantage of FTICR instrumentation is its size. A typical external source FTICR instrument requires a *minimum* of about 100 square feet of floor space. If the magnet is unshielded, then even more space is required to ensure that the fringing fields do not affect unsuspecting people—people with metallic implants such as pacemakers are especially at risk—or cause problems with computer or other electronic equipment.

Regular maintenance is a crucial issue for FTICR instrumentation equipped with a superconducting magnet. To remain superconducting, the magnet coils must be kept below their critical temperature (*i.e.*, the maximum temperature above which the material loses its superconducting ability). Liquid helium is used for this purpose, and because of its relatively high cost, a liquid nitrogen (*ca.* 77 K) Dewar is used to jacket the liquid helium Dewar within the magnet, thereby reducing substantially the rate at which the liquid helium is lost from the magnet. A typical superconducting magnet consumes between 80–150 liters of liquid nitrogen per week, and between 75–100 liters of liquid helium per month. Some provision must be made for filling the magnet with the appropriate cryogens on a regular basis. If any portion of the magnet coils lose their superconducting ability (*i.e.*, become resistive), then the liquid helium will boil rapidly because of Joule heating, resulting in a violent eruption known as a quench. In some cases, a quench will not permanently damage the magnet. However, in magnets of older design, a quench could result in a portion of the magnet being blown out. Such a situation would ruin the magnet, but more importantly anyone in the vicinity of the explosion could be hurt. Even in a best case scenario, a quench will result in about one week of downtime, and several thousand dollars will most likely be spent make the magnet operational again.

Dynamic Range

Currently, the dynamic range of the technique is rather limited ($\sim 10^4$) compared to other types of mass spectrometry (10^6–10^9). For the types of experiments for which FTICR was originally employed, dynamic range was not much of a concern. However, as FTICR takes a more central role in analytical mass spectrometry, such a feature will have to be improved. As mentioned in Chapter 1, a number of groups have already begun work on analyzer cells with potential for 10^8 dynamic range.

Operation at Ultra-High Vacuum

Finally, another often cited disadvantage of FTICR is the requirement for ultra-high vacuum to reap the full benefit of the technique. Use of an atmospheric pressure ionization source (*e.g.*, ICP, glow discharge, ESI, *etc*.) requires an external source instrument with good differential pumping. Such a source adds to the complexity, cost, size, and maintenance of the instrument.

Motions of Ions in a Magnetic Field

Fundamental FTICR Equations

If a charged particle is placed in a magnetic field with some velocity component that is perpendicular to the direction of the field, the particle will experience an inwardly directed force known as the Lorentz force (see Figure 2–2). In the absence of an electric field, the expression for the calculation of the Lorentz force experienced by an ion is shown in Equation 2–1;

$$\boldsymbol{F}_L = q\boldsymbol{v}\times\boldsymbol{B} \qquad \textbf{2-1}$$

where q is the charge of the ion, **v** is its velocity, and **B** is the magnetic flux density, or as it is more commonly known, the magnetic field strength. The cross product of **v** and **B** in Equation 2–1 indicates that only those velocity components perpendicular to the magnetic field contribute to the Lorentz force.

A positive ion undergoing cyclotron motion is depicted in Figure 2–2. In this figure, the ion is shown to orbit in a clockwise fashion. If the ion were negative, it would orbit in a counterclockwise fashion as indicated by Equation 2–1 for the case when q is negative.

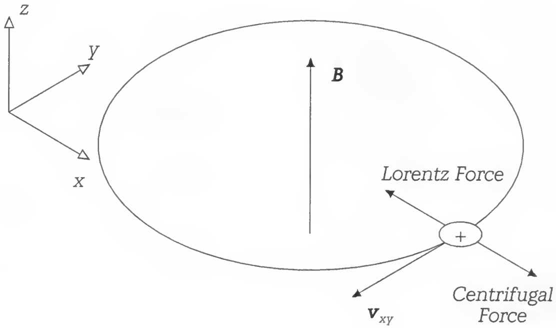

Figure 2-2
Depiction of motion of an ion in a magnetic field. When the inwardly directed Lorentz force equals the outwardly directed centrifugal force, a stable "orbit" is achieved.

The centrifugal force for an object undergoing circular motion is shown in Equation 2-2, where m is its mass, r is the distance of the object from the center of rotation, and v is the velocity.

$$F_C = \frac{m \cdot v^2}{r} \qquad \textbf{2-2}$$

When the centrifugal force is equal to the Lorentz force, the ion achieves a stable orbit, and the expressions in Equation 2–1 and Equation 2–2 can be equated as shown in Equation 2–3.

$$\frac{mv}{r} = qB \qquad \textbf{2-3}$$

The quantity v/r in Equation 2–3 is equal to the angular frequency, ω, which is the number of radians swept out by the ion per unit time. By substitution of this quantity into Equation 2–3 and rearranging, the famous cyclotron equation is obtained (Equation 2–4).

$$\omega_c = \frac{qB}{m} \qquad \textbf{2-4}$$

Angular frequency (radians·s^{-1}) can be converted to linear (or direct) frequency (Hz = cycles/s) by dividing by 2π, because there are 2π radians in one "cycle" (period). Equation 2–5 is the cyclotron equation expressed in terms of SI units.

$$\nu_c = \frac{qB}{2\pi m} \qquad \textbf{2-5}$$

The cyclotron equation reveals an interesting property about ions in magnetic fields: the cyclotron frequency of an ion depends only on the ion's m/z and the applied magnetic field strength. This property is one of the reasons that FTICR is capable of measuring spectra with ultra-high mass resolving power. With double-focusing high-resolution sector based mass spectrometers, the accuracy with which an ion's m/z can be determined depends on how precisely the ions can be focused on the basis of kinetic energy. By contrast, an ion's cyclotron frequency is independent of its kinetic energy. Additionally, the m/z of an ion is determined from its cyclotron frequency, and since frequency is the most accurately measured physical quantity,[89] FTICR provides a very accurate m/z determination.

The discussion of ion motion thus far has been limited to a two dimensional case. In an actual experiment, ions are free to move in three dimensions, and a more complete understanding of their motion requires extension of the preceding analysis.

In the case of an FTICR experiment, ions must be trapped in order to be mass analyzed. Trapping is accomplished via the use of a Penning ion trap, or as it is more commonly known in FTICR, an analyzer cell. A typical analyzer cell consists of the following essential components: front and rear trapping electrodes, one pair of excitation electrodes, and one pair of detection electrodes. Figure 2-3 is an example of an open-ended analyzer cell.

The motion of ions in a Penning ion trap can be likened to that of beads on a string, with the bead representing the ion, and the string

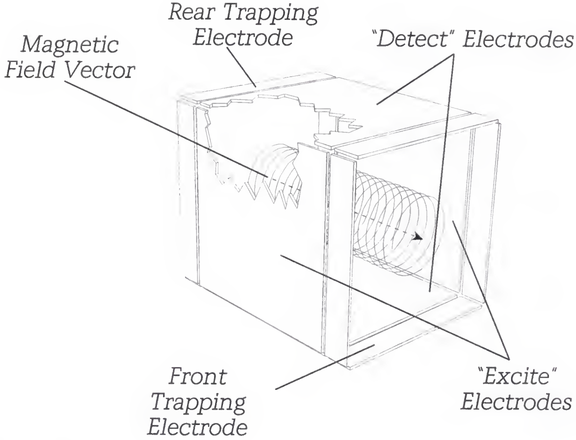

Figure 2-3
Representation of an FTICR open analyzer cell showing relative placement of various electrodes and orientation with respect to the magnetic field vector.

representing the magnetic field vector. In the case of the beads, they are free to move along the string or to rotate about it, but they cannot move in directions perpendicular to it (see Figure 2–4). Although the beads are trapped radially by the string, they can escape the string at its endpoints unless some provision is made to "trap" them.

For ions in an FTICR analyzer cell, the combined action of the Lorentz and centrifugal forces serves to prevent an ion from escaping radially in a manner analogous to the string in the example with the beads. However, as in the case with the beads on the string, some provision must be made to keep the ions from escaping the cell axially (*i.e.*, along the direction of the magnetic field vector or z axis). The trapping electrodes depicted in

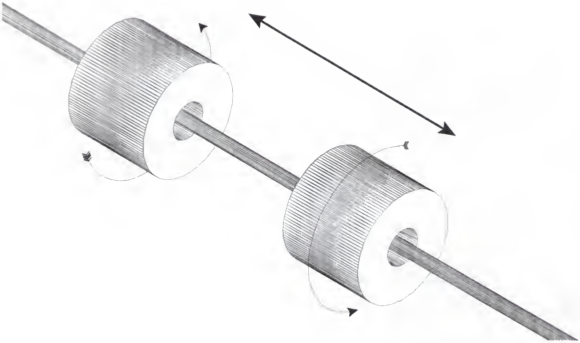

Figure 2-4
The motion of beads on a string can be used to visualize the movement of ions in Penning trap.

Figure 2-3 serve this purpose. By applying a potential to each trapping electrode that is of the same polarity as that of the ions, the ions are prevented from escaping along the z axis. This trapping potential results in a quadrupolar electric field as depicted in Figure 2-5. The introduction of the

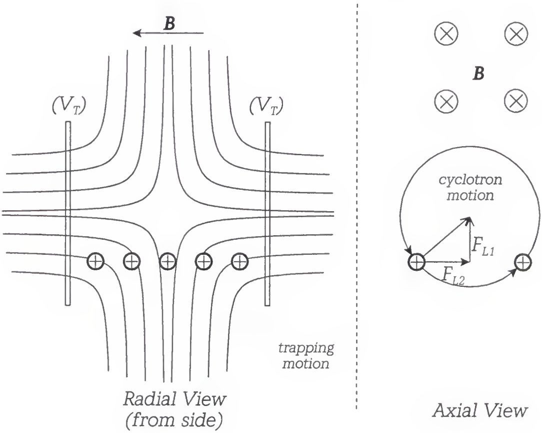

Figure 2-5
Depiction of the quadrupolar electric field lines that result from the electrostatic trapping potential applied to each electrode.

trapping potential gives rise to two additional periodic motions: magnetron motion and trapping oscillation (or z axis motion).[90]

To a good approximation, the forces—and hence, the resulting ion motions—that are parallel and transverse to the magnetic field vector may be analyzed as though they were independent of each other. With the introduction of a trapping potential, ions are squeezed to the center of the trap, where the trapping electric field varies approximately linearly with position along the z axis. This linear variation in electric field results in periodic motion that is analogous to a mass on a spring, where the restoring force is linearly related to position (Hooke's law). Just as the mass on a spring oscillates with a natural frequency, the ions in a Penning trap also exhibit oscillatory behavior. The expression for the trapping frequency varies slightly with trap geometry. There are several equivalent expressions for the magnetron frequency and trapping frequency in the literature. Equation 2-6 is a common form of the equation that describes the angular trapping frequency for a cubic cell;

$$\omega_T = \sqrt{\frac{2\alpha q V_T}{ma^2}} \tag{2-6}$$

where q is the charge of the ion, α is a constant that depends on trap shape (e.g., $\alpha = 1.39$ for a cubic trap), V_T is the trapping voltage, m is the mass of the ion, and a is a characteristic trap dimension, which in the case of the cubic cell is the length of one side. It is worth noting that no expression for magnetic field strength is shown in this equation, thereby reaffirming the earlier statement that the axial and radial forces are independent of each other to a good approximation.

The magnetron motion has an angular frequency described by Equation 2–7,

$$\omega_- = \frac{\omega_c}{2} - \sqrt{\frac{\omega_c^2}{4} - \frac{\omega_T^2}{2}} \qquad \textbf{2-7}$$

where ω_c is the angular cyclotron frequency. Because the magnetron frequency results in a downward shift of the cyclotron frequency, it is given a "–" subscript as shown in Equation 2–7. The origin of the negative shift can be understood by looking at Figure 2–5. In this figure, the electric lines of force are directed away from the electrode surfaces. It is well known that a charged particle in an electric field experiences a force. By convention, the direction of the force is away from the electric field lines for positive charges, and towards the field lines for negative charges. Equation 2–8 is the expression for the force exerted on a charge by an electric field.

$$\boldsymbol{F_E} = q\boldsymbol{E} \qquad \textbf{2-8}$$

In this equation the electric charge is denoted by q as usual, and **E** is the electric field strength. Looking at Figure 2–5, it is clear that the ions experience an outwardly-directed radial force that is the result of the trapping potential. Marshall has described this effect by analogy to a balloon, where squeezing the balloon at each end results in bulging at the middle. The ions experience a static electric force at any point in the cell; however, the component of the electric force that is responsible for the outwardly-directed radial force becomes more severe as the ions approach the center of the analyzer cell as shown in Figure 2-5. In the axial view of this figure, the Lorentz force is separated into two perpendicular components, $\mathbf{F}_{L1}$ and $\mathbf{F}_{L2}$. Clearly, the radial electric field opposes the $\mathbf{F}_{L1}$ component of the Lorentz force, resulting in decreased trapping ability and an acceleration that opposes the cyclotron motion, thereby shifting the cyclotron frequency to a lower value. This effect is greatest at the center of the cell.

The reduced cyclotron frequency is denoted by ω_+ because of the complementary relationship shown in Equation 2-9.

$$\omega_c = \omega_+ + \omega_- \qquad \textbf{2-9}$$

By combination of Equations 2-7 and 2-9, the expression for the reduced cyclotron frequency takes the form shown in Equation 2-10.

$$\omega_+ = \frac{\omega_c}{2} + \sqrt{\frac{\omega_c^2}{4} - \frac{\omega_T^2}{2}} \qquad \textbf{2-10}$$

The quantities under the square root signs in Equations 2–7 and 2–10 have an important implication for the upper mass limit in FTICR. Because ω_c is proportional to 1/m, whereas ω_T is proportional to $\sqrt{\frac{1}{m}}$, it is clear that the results obtained for Equations 2–10 and 2–7 will become imaginary at sufficiently high m. This result physically corresponds to the outwardly–directed radial electric field becoming so strong, that it overcomes the Lorentz force, and the ions are permanently lost from the analyzer cell. The mass at which this condition occurs for a given set of parameters is known as the critical mass, m_{crit}. The condition which must be satisfied for this effect to occur is shown in Equation 2–11.

$$\frac{\omega_c^2}{4} - \frac{\omega_T^2}{2} = 0 \qquad \textbf{2-11}$$

Because the trapping frequency increases with respect to the trapping voltage, it can be inferred from Equation 2–11 that the maximum observable mass in FTICR decreases as the trapping voltage is increased. A more useful equation for the determination of the critical mass is shown in Equation 2–12,

$$m_{crit} = \frac{a^2 B^2}{4\alpha V_T} \qquad \textbf{2-12}$$

where, '*a*' is a characteristic trap dimension, B is the magnetic field strength, α is the geometry factor, and V_T is the trapping voltage. As shown in Equation 2-12, the critical mass increases with the square of the applied magnetic field (*i.e.*, $m_{crit} \propto B^2$), so that a small increase in magnetic field strength results in a large increase in the critical mass, one of the many advantages of a higher magnetic field.

Experimental FTICR Sequence

As depicted in Figure 2-6, a basic FTICR experiment consists of five principal steps: ionization, trapping, excitation, detection, and application of

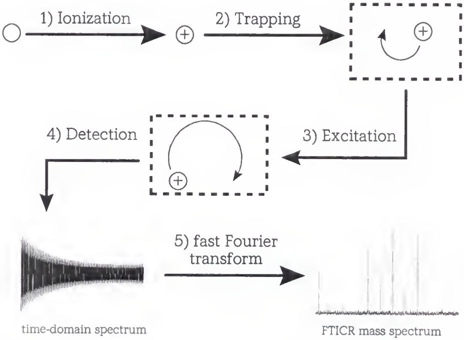

Figure 2-6
Principal steps in the acquisition of a mass spectrum by the FTICR technique

the fast Fourier transform to obtain the spectrum. The remainder of this section discusses each of these topics.

Ionization

With the completion of the work presented in this dissertation, every commonly applied ionization source in mass spectrometry has been used with FTICR instrumentation. Some of the more common ionization methods are shown in Table 2–2. The inductively coupled plasma as an ionization source will be discussed in Chapter 3.

Table 2–2

Common Ionization Methods in Mass Spectrometry

EI	electron impact
CI	chemical (*i.e.,* use of a reagent gas such as methane)
LD	laser desorption (LD)
MALDI	matrix assisted laser desorption
FAB	fast atom bombardment
ESI	electrospray
APCI	atmospheric pressure chemical ionization
GD	glow discharge
ICP	inductively coupled plasma

Depending upon the location of the ionization source, FTICR instruments are categorized as being either internal or external source. In the internal source instruments, the ionization source is positioned inside the high magnetic field very near the cell. Ionization of the sample occurs either directly in the cell or very close to it. High detection efficiency is the main advantage of internal source instruments. The primary disadvantage of internal source instruments is the limitation imposed by the high vacuum requirements of FTICR. Use of high pressure sources (*e.g.*, ESI, glow discharge, *etc.*) with an internal source instrument requires a somewhat complex pumping arrangement, as shown in Figure 2-7. Additionally, the ionization source is no longer easily accessible, so routine maintenance becomes much more difficult, and viewing of the source to ensure reliable operation is precluded. In terms of pressure, internal sources based on EI, CI, and MALDI ionization do not present great difficulties because of the their low gas loads. For sources with high gas loads (*e.g.*, ESI, APCI, ICP, *etc.*) however, an external source design is usually preferable.

In the external source design, the ionization source is placed outside the strong magnetic field gradient. Through the use of a series of conductance limits, several stages of differential pumping, and a system of ion transfer optics, ions can be sampled at atmospheric pressure and detected at pressures below 10^{-9} torr, a difference of almost 12 orders of magnitude. Figure 2-8 is a schematic representation of an FTICR instrument equipped with an externally located ICP source. In the instrument depicted in this figure, the ion transfer optics consist of a series of electrostatic lenses. To

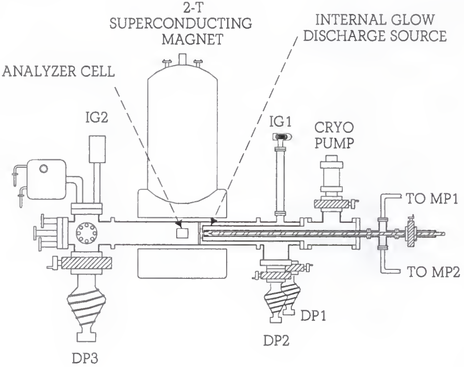

Figure 2-7
Schematic representation of an internal glow discharge source for an FTICR instrument. Note that the source is not easily accessible.

overcome the magnetic-mirror effect,[91,92] the ions are accelerated to high kinetic energies by the acceleration optics.[93] If the ions were not slowed by the deceleration optics, they would pass through the analyzer cell without being trapped. Additional methods have been used for ion transfer from external sources: *e.g.*, multipoles consisting of quadrupoles[94] or octopoles[95] operating in the rf-only mode, and wire-in-cylinder electrostatic ion guides.[96]

Clearly, the biggest advantage of external source systems is the tolerance for high pressure sources. In terms of disadvantages, external ion sources generally require more space than internal sources, and there is the additional complication of the ion transfer optics which must be tuned for optimal signal. For uncharacterized sources, this optimization can literally take several weeks or longer before optimum conditions are attained. Finally, an additional factor which must be considered with external sources arises from the time-of-flight effect, where ions of lower m/z arrive at the analyzer cell first. For most FTICR experiments, this effect is not a problem, but it should be considered.

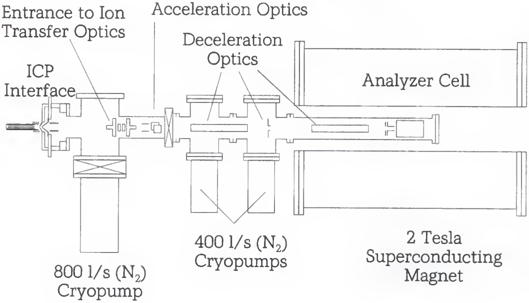

Figure 2-8
Schematic representation of an external source ICP–FTICR instrument showing pumping arrangement and ion–transfer optics system.

Ion Injection and Trapping

The trapping process employed in FTICR varies depending upon the source location. Ions formed by an internal source have a distribution of velocities that can be influenced by application of electrostatic fields if necessary. On average, these ions will have some velocity components perpendicular to the magnetic field, therefore they will be trapped radially by the magnetic field, and axially upon application of an electrostatic trapping field as discussed earlier.

Unlike the passive nature of trapping ions from an internal source, trapping externally injected ions requires additional effort. The most common method of trapping externally generated ions in FTICR, sometimes referred to as *accumulated trapping*, involves the use of a collision gas. With this method, the externally generated ions are directed to the analyzer cell via the ion-transfer optics. Prior to their entering, a collision gas is introduced into the cell that raises the base pressure to about 10^{-5} torr. Upon entering the high pressure environment in the analyzer cell, the ions undergo a series of collisions that serve to reduce their kinetic energy, whereby they tend to collapse to the center of the analyzer cell. Figure 2-9 is a typical FTICR event sequence incorporating accumulated trapping.

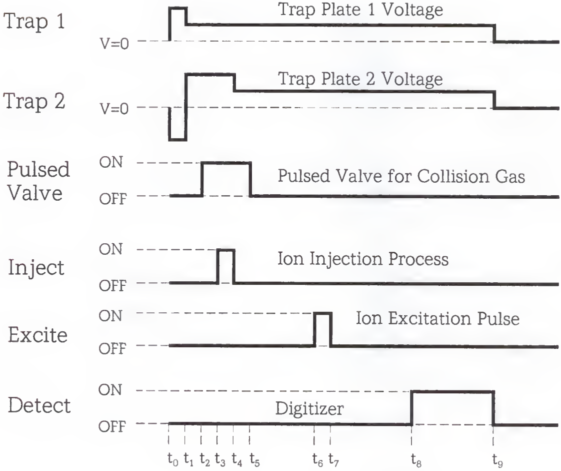

Figure 2-9
Accumulated-trapping event-sequence for an FTICR experiment.

The first event in almost every FTICR experiment is the *quench* pulse. By applying a voltage of +V to one trap electrode and -V to the other, any ions present in the cell will be eliminated regardless of their charge. Omission of the quench pulse would result in unwanted ions that reduce the holding capacity of the analyzer cell. In Figure 2-9, the quench pulse is started at time t_0. At time t_1, the voltage on the second trap electrode is raised to a level slightly above that placed on the first trap plate. This slight offset in voltage is useful for trapping ions, but it distorts the quadrupolar field and results in undesirable frequency shifts that degrade mass accuracy. Therefore, as shown in the event sequence, the trap electrodes are restored to a uniform voltage prior to detection for best results. Next, the collision gas is introduced into the cell via a pulsed valve. After the pulsed gas has raised the cell pressure, the ion injection optics are activated to pulse in the sample at time t_3. A time delay is placed between the inject event and the excite event to allow for "cooling" of the ions via collisions. This delay is also necessary to give the vacuum system time to reduce the base pressure to levels that are suitable for FTICR detection. Finally, the ions are excited via application of resonant rf energy, and after a short delay, the resulting time-domain signal is detected.

The accumulated trapping method has several features advantageous to FTICR. It is well-suited for trapping ions of widely varying m/z values and/or kinetic energies. Additionally, ions are injected on-axis, a factor which some contend has pronounced effects on analytical performance. The major drawback to accumulated trapping is a reduction in duty cycle because of the long pumping delay between the injection and excitation events. Additionally, if cryopumps are used in the high vacuum region, the extra gas load imposed by the collision gas decreases the time between pump regenerations, thereby resulting in increased downtime.

An alternative method for trapping externally formed ions, which incidently has been commercially implemented by Bruker Daltonics, is known as side-kick trapping. To effect side-kick trapping, a pair of closely spaced hemispherical electrodes is placed at the entrance side of the analyzer cell. By imposing a potential difference between the electrodes, ions entering the analyzer cell on-axis experience a force described by Equation 2-8 which gives them a large velocity component perpendicular to the magnetic field vector, thereby converting axial motion into cyclotron motion.

Side-kick trapping requires no pulsed gas to cool the ions, therefore, it does not impose the restriction of a pumping delay. This feature results in a good duty cycle (~1 sec/spectrum) compared to the method of accumulated trapping (~10 sec/spectrum).

The side-kick method has some serious weaknesses. Of these, the one most relevant to the work presented in this dissertation is inability to trap ions with a wide range of kinetic energies. This drawback precludes its use with sources that do not produce monoenergetic ions (e.g., ICP). Second, it will not effect trapping of ions with high kinetic energies. Such ions will have large cyclotron radii when trapped, and unless some provision is made (e.g., introduction of a collision gas), these ions will be lost during the excitation process. If a collision gas must be introduced anyway, then accumulated trapping should be used.

Ion Excitation in FTICR

There are many references that discuss the fundamental process of excitation in FTICR.[97,98,99] When an ion experiences an oscillating electric field, it will absorb energy if its cyclotron frequency is resonant with the electric field. The radius at which an ion orbits can be determined from Equation 2–13,

$$r = \frac{1}{qB}\sqrt{2mkT} \qquad \textbf{2-13}$$

where, q is the charge, B is the applied magnetic field strength, m is the mass of the ion, k is Boltzmann's constant and T is the Kelvin temperature of the ion. Equation 2–13 can be readily derived from Equation 2–3, and Equation 2–14 which relates the translational energy of an ion to its temperature.

$$kT = \frac{mv_{xy}^2}{2} \qquad \textbf{2-14}$$

As shown in Equation 2–13, the cyclotron radius of an ion can be increased by increasing its temperature/kinetic energy. In addition to increasing an ion's cyclotron radius, excitation simultaneously achieves spatial coherence, an important feature for detection in FTICR. The excitation process is depicted in Figure 2-10.

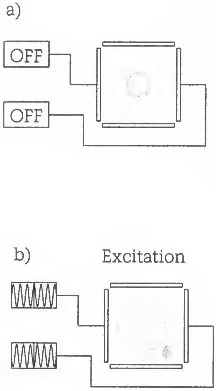

Figure 2-10

a) The ions have random orbital phase, and are located far from the detection electrodes initially.

b) In the presence of a resonant oscillating electric field, the ions will absorb energy and increase their orbital radius while simultaneously achieving *spatial coherence*.

The discussion thus far has focused on resonant excitation, but in practice, off-resonant excitation must also be considered for optimum analytical performance. A particularly useful discussion of this concept was given by Heck *et al.*[100]

In addition to being a prerequisite for detection, ion excitation is also used for a variety of other reasons in FTICR. In the study of reaction mechanisms for example, ion excitation can be used to "heat" an ion in order to drive an ion-molecule reaction, a process akin to heating a reaction mixture in a beaker with a flame. Additionally, ion excitation can be used to rid the analyzer cell of unwanted ions with high specificity by increasing their cyclotron radius to such a large degree, that they strike an electrode surface and are neutralized. Some of the commonly used modes of ion excitation in FTICR are briefly discussed below and summarized in Figure 2-11.

Single-Frequency Excitation

In this method, an rf pulse of very narrow frequency is applied to the excitation electrodes for a very short duration (usually < 100 μs). The time-domain and frequency domain representations of a short pulse are shown in Figure 2-11a. The half width of the frequency domain peak is inversely related to the pulse duration. Single frequency excitation is used in

FTICR to eject unwanted peaks with excellent specificity. Additionally, it is also used to excite the ions for detection in heterodyne experiments.

Chirp Excitation

Also known as frequency sweep excitation, chirp excitation[101] was demonstrated soon after the first FTICR publication. In this method, a series of frequencies are scanned at a rate that is linear in time. The chirp results in all ions being excited to approximately the same orbital radius. All ions are not excited simultaneously with a chirp, but the total excitation time is very short (typically, a few ms).

Figure 2-11b is a time and frequency domain representation of a chirp waveform. The chirp does not give a flat power profile, but it is adequate for most purposes. Despite its age, the chirp is still probably the most widely employed method of ion excitation in FTICR.

SWIFT Excitation

The most versatile method of ion excitation in FTICR, *stored waveform inverse Fourier transform* (SWIFT) excitation was developed in 1985.[102] The SWIFT technique allows for very precise control of ion excitation in FTICR. With this method, a frequency domain power spectrum is specified initially by the user. The inverse Fourier transform is used to determine the corresponding time domain spectrum.

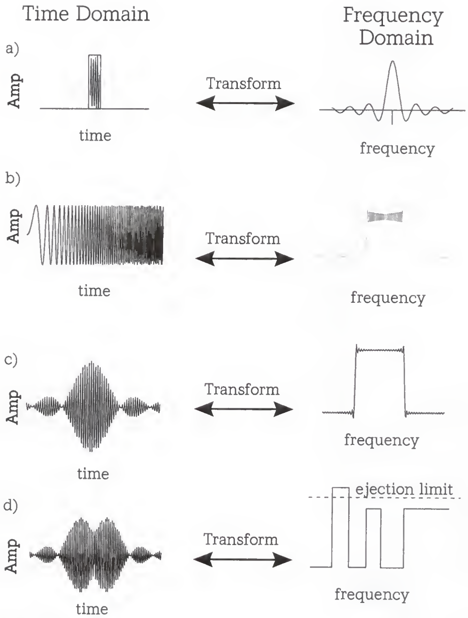

Figure 2-11

a) single frequency excitation
b) chirp excitation
c) SWIFT excitation
d) SWIFT excitation and selective ejection of unwanted species

The time domain spectrum is then downloaded to an arbitrary waveform generator (AWG), whose output is directed to the excitation electrodes of the analyzer cell as usual.

In addition to offering very precise control of the excitation/ejection of ions, the SWIFT technique excites all ions simultaneously. This feature combined with the simultaneous detection makes FTICR a true multiplex method.

As shown in Figure 2-11c, SWIFT results in frequency domain waveforms that are very uniform. However, even with the SWIFT technique, the power at the edges of a frequency window is always slightly uneven, a consequence of the Gibbs phenomenon.[103] Figure 2-11d is an example of how SWIFT can be used to excite some m/z values for detection, eject unwanted ions, and ignore the remaining ions.

FTICR Detection

After being trapped, ions of a given m/z undergo cyclotron motion with the same orbital frequency, but random orbital phase (see Figure 2-12). In addition to random phase, the initially formed ions typically have a small cyclotron radius.

Detection in FTICR is based upon the principle of electric induction, whereby a current flows through a circuit in response to an accumulation of charge. The current will always flow in such a way that seeks to minimize the charge buildup, a manifestation of Lenz' law. Figure 2-13 illustrates how this principle is relevant to FTICR detection.

$$\frac{\partial \Theta}{\partial t} = \omega_c = \frac{\|\mathbf{v}\|}{r}$$

$$\frac{\partial \mathbf{s}}{\partial t} = \mathbf{v}$$

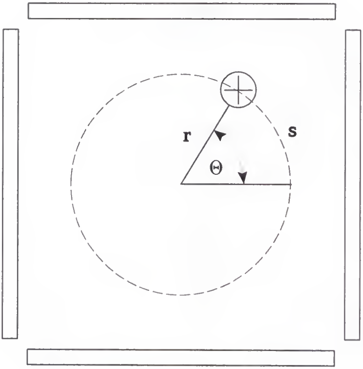

Figure 2-12
Depiction of ICR orbital phase.

The process of detecting an FTICR signal is portrayed in Figure 2-14. In Figure 2-14a, the ions are initially trapped with a relatively small kinetic energy. No net signal is observed because the ions are too far away from the detection electrodes, but more importantly, they are not spatially coherent. Even if the ions were closer to the detection electrodes, no net signal would be observed because induced charge from ions on one side of the cell would be canceled by ions on the other side of the cell. In Figure 2–14b, rf energy is applied to the "excite" electrodes of the FTICR analyzer cell. At this point, the spatially coherent ion packet acts as an ensemble, inducing a net signal in the detection electrodes. In Figure 2–14c, the excitation is turned off, and the resulting signal is digitized.

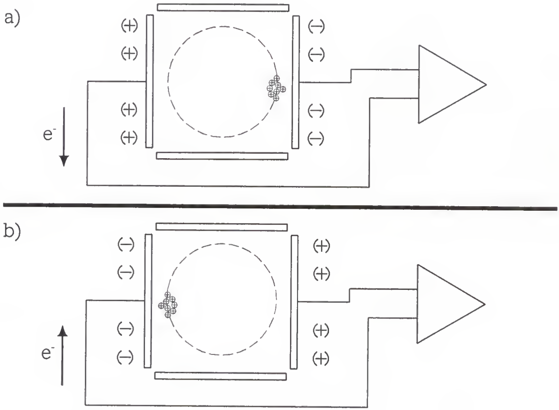

Figure 2-13
Electric induction in FTICR.

a) As the ion ensemble approaches the right electrode, electrons flow from left to right in the circuit to neutralize the induced charge.

b) The electrons flow in the opposite direction as the ions approach the left electrode.

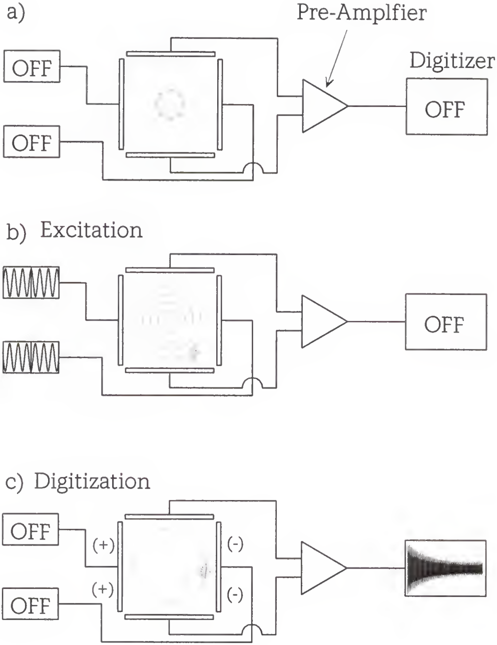

Figure 2-14

Process of Signal Detection in FTICR

a) Initially, ions have a small cyclotron radius and random orbital phase.

b) rf energy is applied to excite the ions to a larger orbit and bring about spatial coherence.

c) The induced charge (image current) is detected.

A short delay between the excitation and detection events is necessary, otherwise the detected signal will be distorted by the excitation signal.

Although an image current is induced in the detect electrodes, it is experimentally easier to measure voltage. By directing the current through an impedance, conversion to a voltage is readily accomplished. After voltage conversion, the resulting signal is amplified and subsequently sampled by the digitizer.

The digitized, time-domain FTICR signal is usually referred to as a transient, or free ion decay (FID) spectrum. Consisting of a series of voltages at discrete times, the time domain spectrum is converted to the frequency domain by application of the FFT routine. The frequency domain spectrum consists of a series of amplitudes as a function of discrete frequency values. This spectrum is then converted to the mass spectrum by application of a calibration equation such as that shown in Equation 2-15, where C_1 and C_2 are constants, and f is the measured ICR frequency for an ion with mass-to-charge ratio m/q.

$$\frac{m}{q} = \frac{C_1}{f} + \frac{C_2}{f^2} \qquad \textbf{2-15}$$

The first term on the right hand side of Equation 2-15 is simply a rearranged form of the cyclotron equation (Equation 2-4). The second term must be included because of the effect of the trapping field and *space charge* effects.

Broadband and Heterodyne Detection in FTICR

Two general modes of detection are employed in FTICR mass spectrometry, broadband and heterodyne. In the broadband mode, the FTICR signal is digitized directly. Broadband mode is used when acquiring a mass spectrum over a wide mass range. Because of the large disparity in cyclotron frequencies of ions, the bandwidth in FTICR experiments can be quite large (several MHz). Typically, the spectral resolution (*i.e.*, Δm for FTICR) observed in broadband spectra is limited by the *digital resolution* of the acquisition system. The digital resolution is simply the bandwidth of the acquisition divided by the number of sampled data points. A smaller value for the digital resolution corresponds to a higher resolving power; thus, digital resolution can be improved in two ways: (1) by increasing the number of sampled points, or (2) by decreasing the signal bandwidth. The number of sampled data points is limited by the digitizer's memory, which can not be increased. However, the signal bandwidth can be decreased by heterodyne detection.

Heterodyne refers to a data collection mode where the analytical signal is mixed with a reference frequency, then sent through a low pass filter before being digitized (see Figure 2-15).

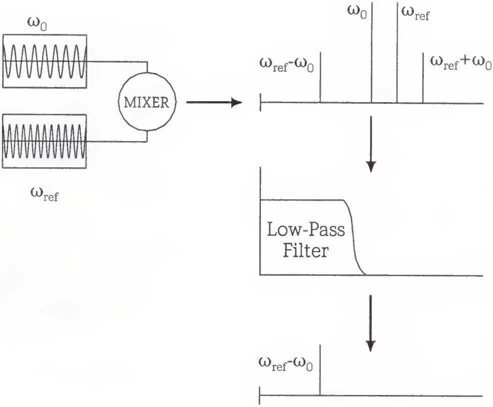

Figure 2-15
Heterodyne Detection in FTICR.
The heterodyne mode of detection is used to reduce the bandwidth of a signal.

Although heterodyne detection decreases the sample bandwidth in an FTICR experiment, a process which results in a concomitant decrease in the observable mass range, other advantages are realized. It is well-known from sampling theory that Johnson noise can be reduced by observation of a signal for a longer time and/or by reducing the bandwidth of the signal. Heterodyne detection effects both of these circumstances simultaneously, because as the bandwidth of the signal is reduced, a lower sampling rate can be used. A lower sampling rate corresponds to a longer sampling time. Longer sampling time is only beneficial when the sample signal lasts longer than the detection period. Table 2-3 contains some broadband and heterodyne parameters for a typical FTICR experiment. Assuming that the FTICR signal persists throughout both detection periods in Table 2-3, the heterodyne detection method will result in a spectral resolving power that is 400 times greater than that which would be observed with the broadband detection scheme for this example. Also notice that the acquisition time increased considerably for the heterodyne mode, while the observable mass range decreased considerably. When digitizers with greater memory capacity become available, they will permit the acquisition of spectra with ultra-high mass resolving power over a much wider range than is currently possible. As

Table 2-3

Comparison of Broadband and Heterodyne Detection

	Broadband	Heterodyne
typical bandwidth	2 MHz	5 kHz
m/z range†	100 – ∞	m ± 1
minimum sampling rate	4 MHz	10 kHz
number of sampled data points	131,072 (2^{17})	131,072 (2^{17})
acquisition time	33 ms	13,107 ms
digital resolution	±15.2 Hz	±0.0381 Hz
relative digital resolution	±400	±1

†In theory, FTICR has no upper mass cutoff, only a lower mass cutoff that is dictated by digitizer and bandwidth considerations. In practice however, ions with cyclotron frequencies of less than 10 kHz are not observable because of 1/f noise.

of the writing of this dissertation, digitizers capable of acquiring 2^{22} ($\sim 4\times 10^{6}$) samples were available.

Conclusions

The intent of this chapter was to give the reader a rudimentary understanding of FTICR, while simultaneously plotting the course of the technique from inception to its present state. As an analytical technique, FTICR mass spectrometry offers many unique advantages in terms of performance. Although modern FTICR mass spectrometers are far superior to their predecessors, the technique still has much room for improvement. Most of FTICR's inherent analytical weaknesses stem from asymmetric electric fields in the analyzer region. Additionally, the dynamic range of the technique needs improvement if it is to realize its full potential. Given the rapid progress of the technique in the past 20 years, efforts to rectify the existing problems are bound to be met with success.

CHAPTER 3
INITIAL ICP-FTICR SOURCE DESIGN

Inductively Coupled Plasma Mass Spectrometry

In less than 20 years,[104] inductively coupled plasma mass spectrometry (ICP-MS) has evolved from a fledgling analytical technique into a premier method for inorganic analysis. This fact is evident by the immense popularity of the technique and its proliferation into almost every sphere where inorganic information is needed. Most of the benefits and some of the characteristics of ICP-MS were described in Chapter 1 of this dissertation. This section is devoted to instrumental aspects of the technique.

As its name implies, ICP-MS is a technique arising from the combination of an inductively coupled plasma (ICP) with a mass spectrometer, whereby the ICP serves as the mass spectrometer's ion source. Aside from a horizontal orientation (as opposed to vertical), the ICPs used with ICP-MS systems are essentially the same as those used in ICP emission spectroscopy.

The plasma itself is a high-energy/high-temperature atmospheric pressure discharge. To *ignite* the plasma, radio-frequency energy is applied to a load coil surrounding a quartz torch with an inert gas, usually argon, flowing through it (see Figure 3-1). The torches are made of quartz because of its ability to withstand high thermal stress. To prevent the load coil from melting, water is usually circulated through it. Next, *seed* electrons are generated, usually by placement of a Tesla coil near the center of the torch-body. As the Tesla coil liberates free electrons by dielectric breakdown of the argon, the electrons undergo a "churning" process that is the result of a rapidly changing magnetic field induced in the coil by the rf energy. These electrons acquire a high kinetic energy, and they subsequently transfer this energy to any species within their vicinity, thereby atomizing and ionizing it in the process that maintains the plasma. Once the plasma has been ignited, the Tesla coil is removed.

To ensure that the rf energy from the generator is absorbed by the plasma rather than being directed back to the generator, or *reflected*, a matching network is employed which varies the impedance of the circuit as necessary.

The gas that sustains the plasma is known by two names, the auxiliary or the support-gas. To help prevent the torch from melting, an outer flow of gas, referred to as either the outer-gas, or the cooling-gas, is directed around the tube carrying the support-gas. Sample is sent to the plasma through a center tube as shown in Figure 3-1. The gas flow carrying the sample is referred to as the center-gas, sample, or aerosol-gas flow. Figure 3-2 is a schematic representation of a typical ICP system.

Figure 3-3, which shows many of the components depicted in Figure 3-2, is a photograph of the ICP instrumentation used throughout most of the work presented in this dissertation. Although solids have been analyzed by ICP-MS, liquid samples are used most frequently with the technique. The plasma is very sensitive to rapid changes in composition; therefore, large amounts of liquid cannot be delivered directly to the plasma. Instead,

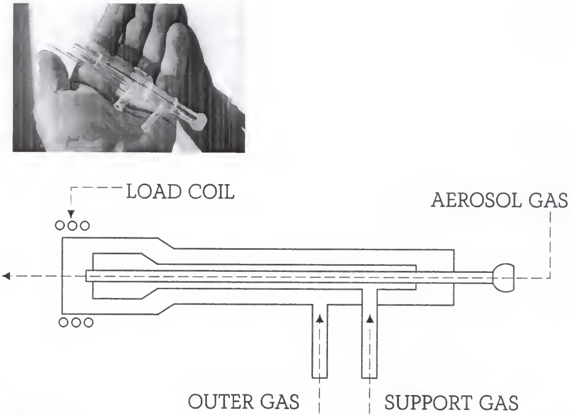

Figure 3-1
Schematic representation of an ICP torch along with a photograph of a Fassel torch.

sample is delivered in the form of an aerosol which is formed by a nebulizer. Figures 3-4 and 3-5 depict the two common types of nebulizers used in ICP-MS. With both types of nebulizers, the sample is dispersed as a fine aerosol, and large particles are condensed and sent to a drain; however, the mechanism of nebulization is quite different between the two.

In a pneumatic nebulizer, liquid sample is introduced through the rear, and a concentric flow of gas through a small orifice results in the sample being dispersed as a fine mist. With pneumatic nebulizers, over 99% of the sample is sent to the drain.

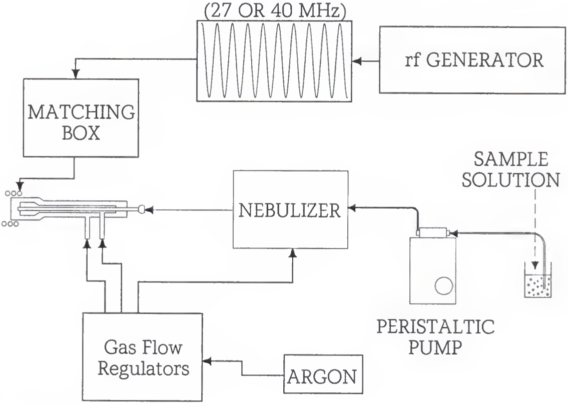

Figure 3-2
Schematic representation of an inductively coupled plasma system.

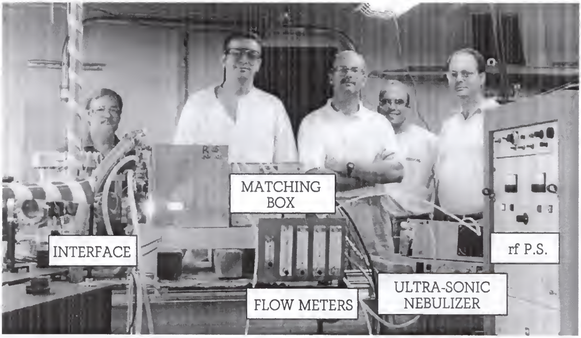

Figure 3-3
Photograph taken at the National High Magnetic Field Laboratory of the ICP instrumentation used to acquire the first analyte signal by ICP–FTICR MS. From left to right, Professor John R. Eyler, Mr. K. Eric Milgram, Professor R. Samuel Houk, Mr. Forest M. White, and Dr. Clifford H. Watson.

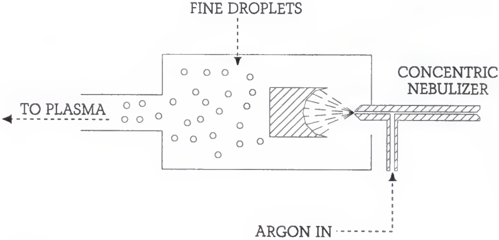

Figure 3-4
Schematic representation of a pneumatic nebulizer.

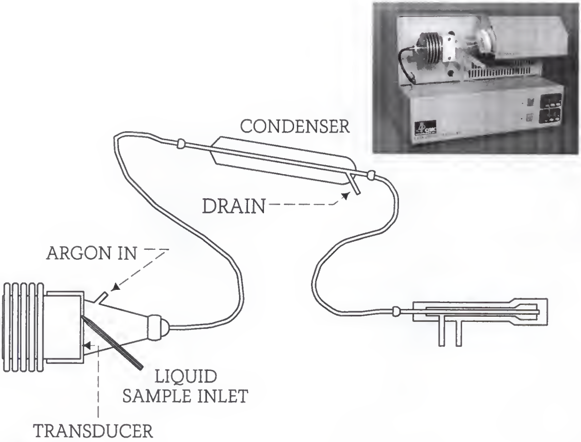

Figure 3-5
Photograph and schematic representation of the ultrasonic nebulizer used in this work.

In an ultrasonic nebulizer, liquid sample is delivered to the face of a piezoelectric crystal, which is also known as a transducer. An rf signal is applied to the crystal at a frequency of 1.4 MHz causing it to vibrate rapidly, resulting in the sample being dispersed as a fine mist. Compared to pneumatic nebulizers, ultrasonic nebulizers can increase sensitivities for some elements by factors of 5–50 because of increased mass transport efficiency. As a consequence of this increased efficiency, the sample must be passed through a condenser before being delivered to the plasma, otherwise the large amount of water carried with it would extinguish the plasma. A peristaltic pump is used to carry the liquid sample to the nebulizer in order to minimize contamination of the sample. Rather than a flow meter, the peristaltic pump used throughout this work was equipped with an indexed, variable-speed control. Figure 3-6 is a plot of flow rate versus index setting for this pump. When the pneumatic nebulizer was used, the maximum pump flow rate was usually specified. However, with the ultrasonic nebulizer, flow-rates in the range 0.25-5.0 mL/minute were used.

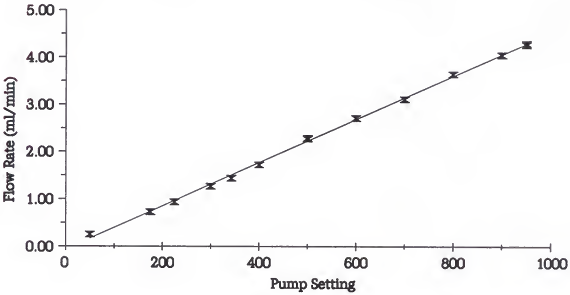

Figure 3-6
Flow Rate as a Function of Peristaltic Pump Setting
With the pump used in this work, the relationship between flow rate and pump setting was very linear.

To extract ions from a plasma, the plasma is placed against a water-cooled, differentially-pumped interface at the appropriate position. Figure 3-7 shows the optimum position for sampling ions from a plasma for ICP-MS.

Figure 3-8 is a schematic representation of a VG PlasmaQuad interface that was used throughout this work. The samplers and skimmers in ICP-MS interfaces are often made of nickel because of its durability, noncorrosive nature, and high melting point. Hole diameters for the samplers and skimmers in ICP-MS are on the order of 0.5-1.5 mm. The region between the sampler and skimmer is maintained at approximately 1-torr to ensure adequate sampling conditions. At this pressure, the hot, atmospheric

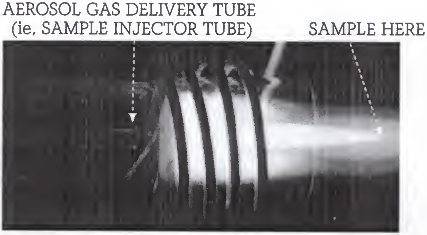

Figure 3-7
Photo showing the optimum location for sampling ions from an inductively coupled plasma for mass spectrometric detection.

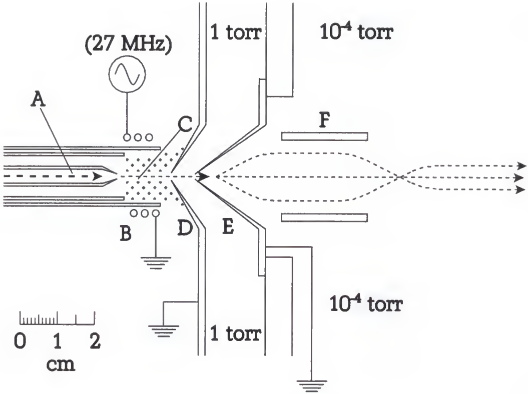

Figure 3-8
Schematic representation of the VG PlasmaQuad interface used in some portions of this work. a) aerosol–gas flow; b) sampler; c) skimmer; d) extractor lens; e) sampled ion trajectory

pressure plasma flowing through the sampler forms a supersonic expansion. The skimmer is placed approximately 7 mm downstream from the sampler in a region known as the *mach bottle*. Because of the supersonic expansion, a shockwave is formed against the skimmer. By placing the skimmer inside the mach bottle, much of the neutral gas can be deflected while retaining much of the sampled ion beam. The sampled ions are then directed to the mass spectrometer for analysis. Only a brief description of ion extraction in

ICP–MS is given here; for a more comprehensive explanation, the reader is directed to a recent review by Niu and Houk.[105]

First ICP–FTICR Source Design

At the onset of this work, combination of an ICP ion source with a FTICR instrument had not been attempted, therefore no appropriate sampling interface existed. In addition to its usual duties, a sampling interface for an ICP–FTICR instrument would have to provide better differential pumping than that required in conventional ICP instruments because of the ultrahigh vacuum requirements of FTICR instrumentation. Given that ESI and ICP sources both operate at atmospheric pressure, we posited that an ESI sampling interface should also be capable of sampling ions from an ICP with suitable modifications. In an ESI source, ions generated by a large electric field (~3 kV) applied to a needle are sampled by placing the needle close to a capillary made of either glass or metal. The ions travel through the capillary where they are desolvated, then they are sampled by a combination of skimmers.

Our decision to focus on ESI sources was made for two reasons. For one, ESI sources had already been constructed for FTICR instrumentation and were commercially available. Additionally, Bruker Daltonics (Billerica, MD) furnished us with such a source that was manufactured by Analytica (Branford, CT). The major factor to be considered in the conversion of an ESI source to an ICP source was the large difference in operating temperatures of the two sources. ESI sources operate at room temperature, whereas ICP sources operate at rotational temperatures of 3000 K or more. Because of the high temperature of the ICP, the capillary normally used for ion sampling in ESI had to be modified. We decided to design and build a water-cooled skimmer to protect the capillary from the intense heat of the ICP. Figure 3-9 is a scale drawing of the skimmer design initially created for this purpose. The channels for cooling water are not shown in Figure 3-9, but are shown in Figure 3-10. The entire assembly actually consisted of two pieces. The piece depicted in Figure 3-10 was constructed of brass because of its ability to conduct heat well and because of its desirable machining properties. The cooling channels were cut with a ball end mill by mounting the piece horizontally on a rotary block. The diameter of the hole at the tip was 0.020" (~0.5 mm). This piece was sealed with a cone shaped piece of copper that was brazed to it. Copper was chosen because of its high melting point. The entire piece was not constructed of copper because of the difficulty in machining copper.

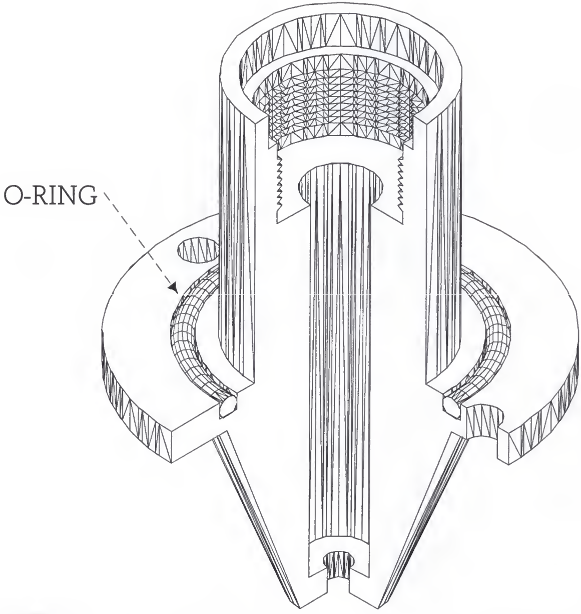

Figure 3-9
3D cutaway of the first skimmer designed to protect the ESI capillary from the intense heat of the ICP.

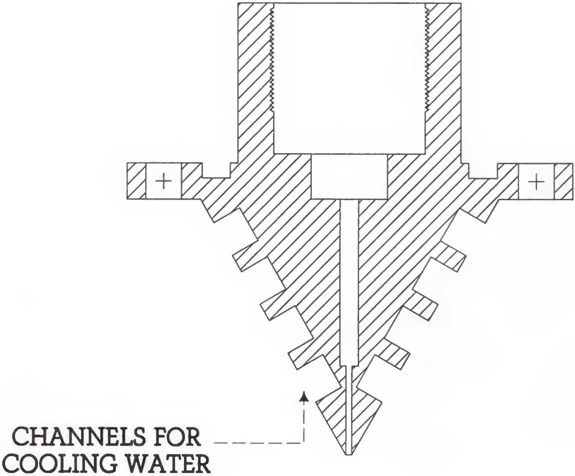

Figure 3-10
Cross-section of the skimmer design for the first ICP-FTICR interface.

Next, a torch holder capable of accurately translating (±0.005") the torch had to be constructed. Figure 3-11 is a drawing of the torch holder design. This torch holder was constructed entirely of Delrin, except for the piece closest to the plasma, which was constructed of Teflon because of its ability to withstand intense heat. Connections for the rf from the matching box to the load coil were made via brass blocks incorporating Swaglok™ compression fittings that mounted on the underside of the torch holder as

All of the assembled components and their relative positions are shown in Figure 3-12. This assembly was then attached to our external source FTICR instrument. Figure 3-13 is a schematic representation of this instrument.

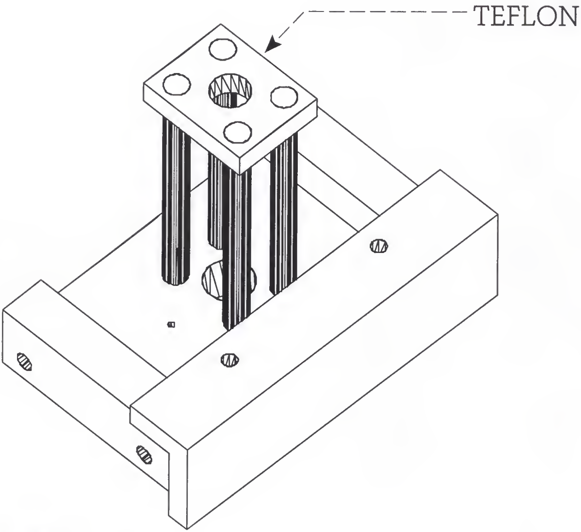

Figure 3-11
3D drawing of the torch holder used for all work presented in this dissertation.

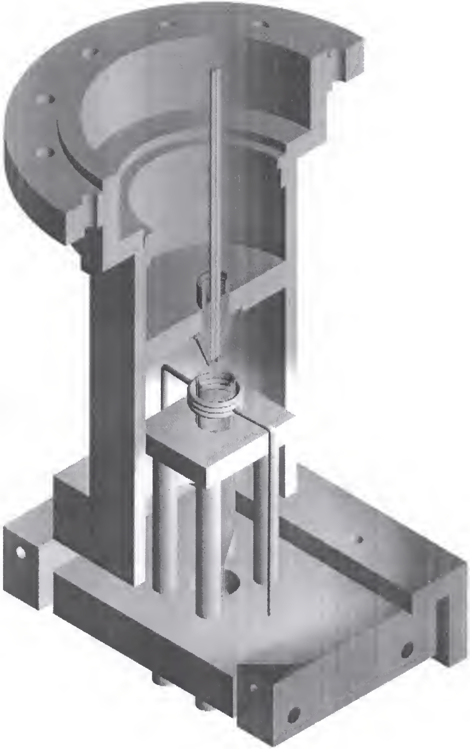

Figure 3-12
3D cutaway of the entire assembly.

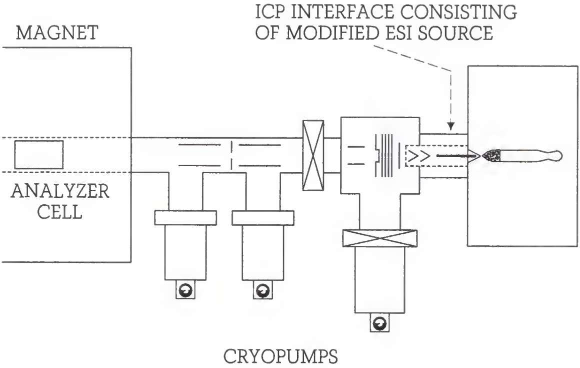

Figure 3-13
Attachment of ESI source to instrument.

When we first attempted to operate this source, we discovered immediately that the ICP could not operate inside the close confines of the ESI housing because of severe arcing. A portion of the housing shown in Figure 3–12 was cut away with a band saw, and the piece was finished by smoothing the rough edges on a lathe.

The experiment was repeated, but the plasma was very unstable. At Professor Houk's suggestion, we enclosed the entire plasma assembly within a metal box connected to an earth-ground. This box, shown in Figure 3–14, improved the operation of the plasma greatly; therefore, it was used in all subsequent experiments.

When this source was bolted onto the instrument, the pressure in the analyzer cell was about 10^{-8} torr, a value which, although not ideal, is suitable for FTICR experiments. The skimmer did not melt, nor did the small sampling aperture close up under the intense heat as we feared. Despite all of our efforts, we were never able to see any signal with this interface. A large *plasma pinch* was noticed, and we attributed the lack of signal to it. Additionally, we were using a pneumatic nebulizer because an ultrasonic one

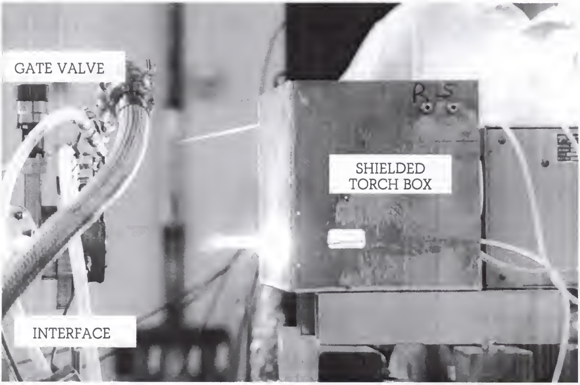

Figure 3-14
Photo taken at the National High Magnetic Field Laboratory of the shielded metal box used for all experiments presented in this dissertation. The interface shown in this photo was not used until later experiments.

was not available, but this was not thought to be the source of the problem because we should have been able to see argon signal irrespective of the nebulizer.

After considering our options, we decided to try a more conventional approach of sampling ions from a plasma. A commercial ICP-MS interface from a VG PlasmaQuad 1 instrument was loaned to us, and this interface was used in subsequent experimental configurations, each of which is described in the next two chapters of this dissertation.

CHAPTER 4
INTERMEDIATE SOURCE DESIGNS

Introduction

As discussed in the conclusion of Chapter 3, we decided to abandon the idea of using a converted ESI source for an ICP–FTICR sampling interface, opting instead to incorporate an interface from a commercial ICP–MS instrument into our design efforts. The work presented in this chapter, which was performed in two stages, highlights the first ICP–FTICR designs incorporating this interface. The first stage of the work, preliminary feasibility experiments, were performed at the University of Florida. The second stage of the work was conducted at the National High Magnetic Field Laboratory (NHMFL).

Given the disregard in the literature for classification of interferences requiring mass resolving power in excess of 10,000, we decided to conduct a classification study. With the aid of a computer program, we enumerated some common interferences in ICP–MS by cataloging them on the basis of *theoretical mass resolving power*. The remainder of this chapter reports the findings of the study, in addition to the outcome of the design efforts.

Experimental Parameters

ICP Parameters

The same standard RF generator and impedance matching network (PlasmaTherm Model HFP2500D, now RF Plasma Products, Voorhees, NJ) were used with all experiments reported in this dissertation. All torches were of the Fassel design[106] with a capillary injector tube. For experiments at UF, the nebulizer was a standard concentric–pneumatic nebulizer (Precision Glassblowing of Colorado, Denver, CO). For experiments at the NHMFL , an ultrasonic nebulizer (Model USN–AT6000+, CETAC Technologies, Omaha, NE) was used with conventional desolvation (*i.e.*, single condenser, no membrane desolvation). As mentioned in the previous chapter, the stability of the plasma was improved greatly by shielding the torch and load coil with an aluminum box connected to an earth ground (see Figure 3–14). Incident rf power, aerosol gas flow rate, and sampling position were selected so that the tip of the initial radiation zone (see Figure 3–7) was located ~1–2 mm upstream from the sampler.

Figure 3–8 is a schematic of the ion sampling interface used with both instruments for this work. As mentioned in Chapter 3, this interface was adapted from a conventional, quadrupole–based, ICP–MS instrument (VG PlasmaQuad I). For instruments at UF and the NHMFL, the gate–valve traditionally used on this interface was removed and replaced with adapter flanges that coupled the water-cooled housing with the FTICR vacuum chambers. The adapter for the UF instrument is shown in Figure 4-1, and the adapter for the NHMFL instrument is shown in Figure 4-2.

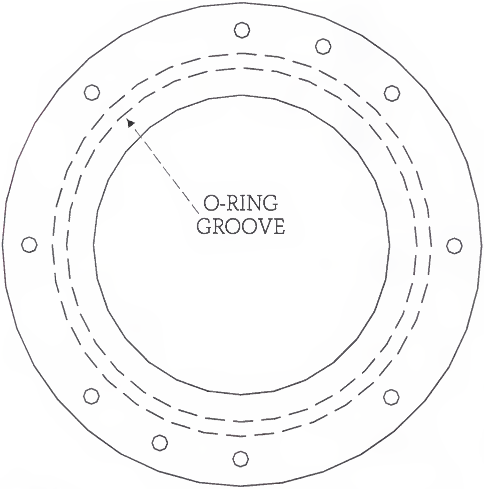

Figure 4-1
Adapter flange for attaching the sampling interface to the UF ICP-FTICR instrument. This adapter was made from a piece of aluminum.

The sampler and skimmer of the interface were both electrically grounded. The extractor lens of the PlasmaQuad I source (labeled D in Figure 3-8) was held at -250 V. The extractor lens and the first ion lens element in the UF instrument were separated by a distance of approximately 15 cm. By contrast, the distance between the extractor lens and the entrance to the wire ion guide in the NHMFL instrument was only approximately 5 cm. Table 4-1 lists all additional ICP parameters.

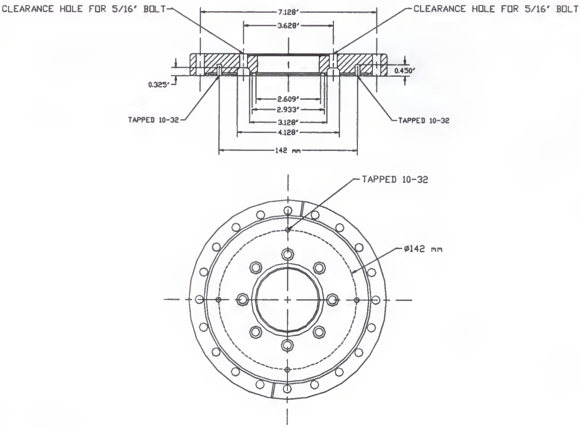

Figure 4-2
Adapter for coupling the sampling interface to the NHMFL instrument. This adapter was made from a standard $4\frac{5}{8}$" to 8" stainless steel knife-edge flange adapter.

Table 4-1

ICP Parameters

RF Generator/Matching Network	
Forward power:	~1.5 kW
Reflected power:	< 20 W
Torch	
Outer gas flow:	15-20 L/min
Auxiliary flow:	0 to 2 L/min
Ultrasonic Nebulizer w/NHMFL Instrument*	
Sample uptake rate:	0.25 - 1.5 mL/min
Heater temperature:	140° C
Condenser temperature:	2° C
Aerosol flow:	0 to 1 L/min
Ion Extraction	
Sampling position:	20 mm from load coil
Sampling cone material/conductance:	nickel/1.0 mm dia.
Skimmer cone material/conductance:	nickel, 0.7 mm dia.
Sampler/Skimmer distance:	7 mm

*The ultrasonic nebulizer was not available for experiments with the UF instrument.

FTICR Instrumentation

The mass spectrometer at the University of Florida was an FTICR instrument consisting of an external source vacuum chamber (MS Model: BioAPEX, Bruker Analytical Systems, Inc., Billerica, MA) and a 2.0 Tesla superconducting magnet (Nicolet, now Finnigan FT/MS, Madison, WI). Ions generated in the source region were transported to the high-vacuum analyzer region via a series of electrostatic lens elements. This instrument will be referred to hereafter as the UF instrument (Figure 4–3).

The mass spectrometer at the NHMFL was a laboratory–constructed instrument, referred to hereafter as the NHMFL system (Figure 4–4).[107] Figure 4–5 is a photograph of the NHMFL instrument. The NHMFL FTICR system was equipped with a 7.0 Tesla, 6" warm–bore, superconducting magnet (Oxford Instruments, Osney Mead, Oxon, England). Designed and assembled in–house, the vacuum chamber was of the external source variety. Ions were generated externally and transported to the ICR analyzer cell by means of an electrostatic wire ion guide.[108] The guide was composed of two

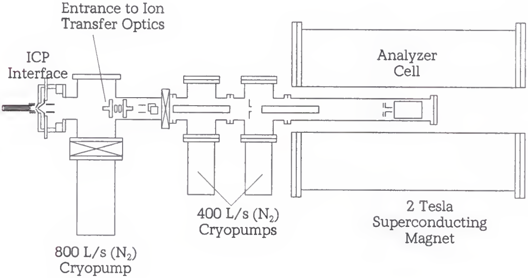
Entrance to Ion Transfer Optics
ICP Interface
Analyzer Cell
400 L/s (N_2) Cryopumps
2 Tesla Superconducting Magnet
800 L/s (N_2) Cryopump

Figure 4-3
Schematic diagram of the world's first operational ICP–FTICR instrument (conceived and located at the University of Florida).

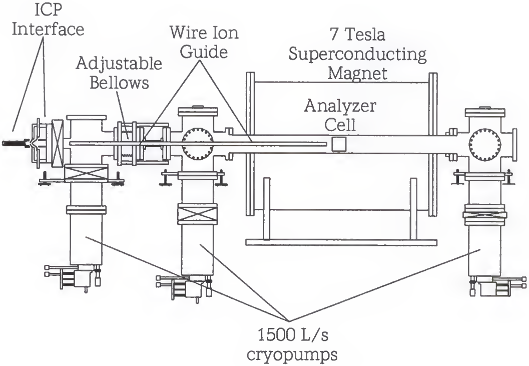

Figure 4-4
Schematic diagram of the NHMFL ICP–FTICR instrumentation.

separate sections: 76.2 cm (30 inches) of perforated stainless steel tubing on the entrance side; 83.8 cm (33 inches) of titanium tubing for the exit side. The guide I.D. was 1.1 cm (0.43 inches) with a wall thickness of 0.89 mm (0.035 inches).

The analyzer cell used with the NHMFL instrument was of open, square cross–section, hexahedral geometry. The open cell design was chosen so that the entire ion beam exiting the wide solid angle of the wire ion guide could be collected. Figure 2–3 is a cut–away depiction of the analyzer cell electrodes drawn to scale.

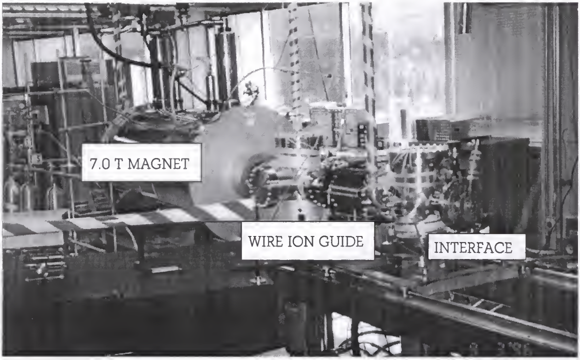

Figure 4-5
Photograph of the NHMFL ICP–FTICR instrument. The adjustable bellows are visible, just above the label WIRE ION GUIDE label.

Data at the NHMFL were collected with the laboratory-constructed "MIDAS" data station.[109] All data acquired with both instruments were processed with WinICR,[110] a data processing package running on a computer equipped with a 133 MHz Intel Pentium™ processor. Time domain spectra were apodized with a centered Gaussian apodization function[111] with the exponent equal to –10 multiplied by the digital resolution, where digital resolution is defined by Equation 4–1.

$$\text{digital resolution} = \frac{\text{spectral bandwidth (Hz)}}{\text{number of data points collected}} \tag{4-1}$$

Mass resolving power for spectra acquired during this work was calculated by dividing the interpolated mass at the peak apex by the peak width at 5% of the peak height ($m/\Delta m_{10\%V}$). The peak apex was determined via a parabolic fit of the 3 highest data points. Table 4–2 lists all relevant FTICR parameters for both instruments.

Reagents and Gases

Industrial grade argon (99.9%) and high purity argon (99.999%) (Bitec Southeast Inc, Tampa, FL) were both evaluated. For these experiments, it was determined that high purity argon offered no distinct advantages over industrial grade argon. Multi–element standards were purchased from Claritas (Metuchen, New Jersey). Single element solutions were prepared with reagent grade solids purchased from Fisher (Pittsburgh, Pennsylvania) and Aldrich (Milwaukee, Wisconsin). These solids were dissolved in the appropriate combination of high purity nitric acid (Fisher) and/or ultra–pure water ($\rho \geq 18$ MΩ·cm) to a final concentration of ~1% HNO_3.

Program Parameters for the Determination of Potential Interferences

Potential interferences, a few of which are listed in Table 1–1, were determined with the aid of a computer program that compared each element

Table 4–2

FTICR MS Parameters[†]

	NHMFL Instrument	UF Instrument
Pressure		
Extractor region pressure:	1×10^{-4} torr	1×10^{-4} torr
Cell pressure:	3×10^{-7} torr	5×10^{-8} torr
Analyzer Cell		
Type of analyzer cell:	square, open	Infinity™ cell
Front trapping electrode (FTE):	+20 to +30 V	+2 V
Rear trapping electrode (RTE):	+5 V > FTE	+0.5 V > FTE
Ion Extraction Parameters		
Wire potential:	−60 V	N/A
Tube potential:	−130 V	N/A
Broadband Detection Conditions		
Size of collected data set:	2^{18} (256 k)	2^{17} (128 k)
Ion accumulation time:	500 ms	500 ms
Detection time:	26 ms	26 ms

[†]N/A indicates that this parameter did not apply for the corresponding instrument.

in the periodic table with a systematically generated list of interferences. Radioactive or unstable elements which have no designated natural abundance (such as plutonium, radon, etc.) were not accounted for by the program. Arbitrarily, isotopes with natural abundances less than 1% were not considered as potential analytes, and all isotopes with natural abundances greater than 0.01% were considered as contributors to potential interferences. Table 4–3 contains a list of all species considered as interferences.

Different criteria have been used throughout this work to describe resolution/resolving power. The use of different criteria was not intentional, but rather the result of different workers in the area of mass spectrometry not adhering to a uniform, consistent definition of mass resolution/resolving power. To avoid further confusion, this author adheres to a set of definitions for mass resolution, mass resolving power, and theoretical mass resolving power (see **Glossary**) throughout this dissertation that he proposed and subsequently submitted to the *Standards and Terminology Committee* of the *American Society for Mass Spectrometry and Allied Topics*.

Table 4–3

Potential Interferences Considered
all stable atomic ions (X^+)
elemental hydrides (XH^+)
elemental argides (XAr^+)
elemental oxides (XO^+)
elemental hydroxides (XOH^+)
elemental nitrides (XN^+)
elemental chlorides (XCl^+)

Note: X represents all stable isotopes with a natural abundance greater than 0.01%.

Results and Discussion

Interferences in ICP-MS Requiring High Resolution Instrumentation

Rather than being all-inclusive, the computer program written to determine potential interferences was designed solely to provide rough numerical estimates of some common interferences. Thus, the true number of interferences which might be encountered in ICP-MS for any element is certainly greater than that predicted by our study. With the computer program, we identified 124 *isobaric* ion interferences requiring greater than 10,000 mass resolving power for separation from the analyte peak of interest. Over 90 of the 124 *isobaric* interferences require mass resolving powers in excess of 50,000 for separation, and more than 30 require mass resolving power greater than 200,000 for separation from the peak of interest. When *polyatomic* ion interferences are also considered, over 1,400 interferences requiring greater than 10,000 mass resolving power were identified.

Preliminary ICP-FTICR/MS Experiments

The UF instrument (Figure 4-3) was used to demonstrate the feasibility of an ICP-FTICR instrument. Figure 4-6a is a background spectrum obtained by sampling ions from the ICP with no aerosol flow.

Although Ar^+ is the dominant spectral feature in Figure 4-6a, other species such as H_2O^+, N_2^+, O_2^+, and Ar_2^+ were also present. With the exception of N_2^+, these additional species are barely visible with Ar^+ shown full scale. Selective ejection of unwanted ions is demonstrated in Figure 4-6b. A single-frequency excitation pulse was used to remove Ar^+ ions from the analyzer cell. The absolute signal magnitudes for the remaining background species (*e.g.* N_2^+ and more importantly, $^{40}Ar^1H^+$) in Figures 4-6a and 4-6b are approximately the same, indicating a highly selective ability to remove unwanted ions. Selective ejection of unwanted ions is just one method that could be exploited to extend the comparatively limited (~4 decades maximum) dynamic range of ICP-FTICR/MS with conventional analyzer cells.

An additional method for removal of Ar^+ ions was also observed with the NHMFL instrument. The Ar^+ ion signal decreased monotonically with respect to ion trapping time. When the ion population was trapped for longer than 10 seconds, the signal due to Ar^+ vanished. Eiden *et al.* noticed a similar effect with a quadrupole ion trap based ICP-MS instrument, and attributed the loss of Ar^+ to charge transfer reactions that occur as a result of argon's high ionization energy relative to other species.[112] We believe that the Ar^+ ion was undergoing charge transfer with H_2O^+, but since we could not observe H_2O^+ in broadband mode because of its high cyclotron frequency at 7 T magnetic field strength, this assumption was not confirmed. Although the remaining H_2O^+ would still contribute to space charge, it would be a trivial matter to remove it with ultra-high precision (because of its small m/z) from the analyzer cell using any of a variety of ejection mechanisms (SWIFT[113], arbitrary waveform generation[114], correlated events[115]) without disturbing the remaining ion population.

The spectrum shown in Figure 4-7 was acquired in heterodyne mode. The mass resolving power demonstrated in this spectrum at the time of the writing of this dissertation was a factor of two higher than that observed with any other ICP mass spectrometer.

Despite the encouraging results shown above, no analytical signal (*i.e.*, signal from an analyte in solution) was ever obtained with the UF instrument in the configuration shown here. Although background species were observed in the mass spectra, we speculated that the sampled analyte ions (which would be in much lower abundance than background species) would be prevented from reaching the ion transfer optics of the Bruker system because of the high pressure in the source region, combined with the large distance the ions had to travel from the extractor lens (Labeled D in Figure 3-8) of the sampling interface.

Analytical ICP-FTICR/MS Results

To test our assumption that ion transfer was the reason we saw no analyte ions, that we attached our source to NHMFL instrument which was equipped with an adjustable bellows assembly. The bellows allowed the position of the wire ion guide to be changed while the system was under

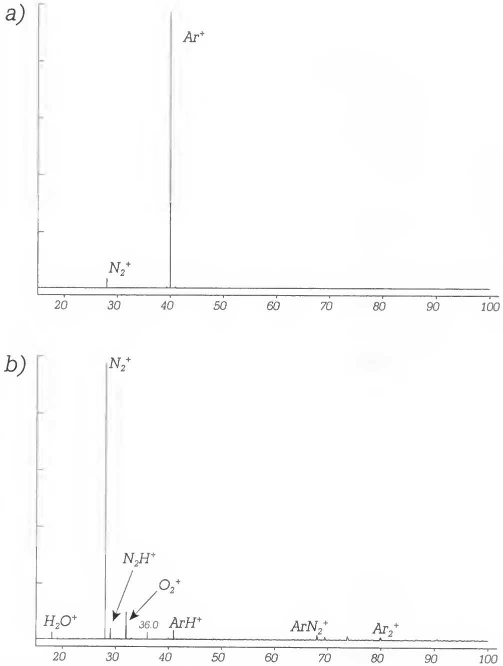

Figure 4-6

a) Preliminary ICP–FTICR broadband spectrum acquired with the UF instrument by sampling the plasma with no aerosol gas flow.

b) ICP–FTICR spectrum showing highly selective ejection of Ar^+, one of the advantages of an ICP–FTICR system.

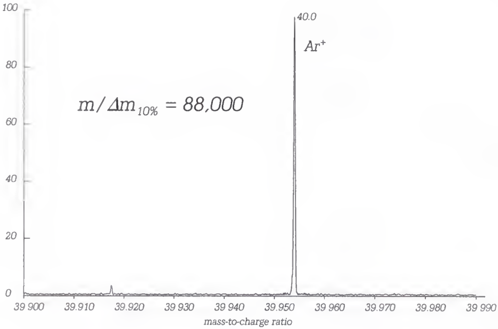

Figure 4-7
ICP-FTICR spectrum of argon demonstrating ultrahigh mass resolving power. The mass resolving power demonstrated in this spectrum was over a factor of two greater than the previous record, which incidently was held by a double-focusing sector mass spectrometer.

vacuum, thereby permitting the entrance to the wire ion guide to be placed very close the extractor lens of the interface. All of our ICP equipment was transported from the University of Florida to the NHMFL in a U-Haul trailer.

The spectrum shown in Figure 4-8, which was obtained by the author and Forest M. White on September 4, 1996, represents the first analytical signal ever obtained by an ICP-FTICR instrument. The analyte solution in this case was a 1,000 mg/L solution of yttrium. Although the S/N was quite poor, this result provided a strong sense of motivation for us to pursue development of an ICP-FTICR instrument, despite the fact that several noted authorities in the area of ICP-MS had stated that such an instrument would not be practical or feasible.

Over the next several days, we improved the sensitivity significantly. In addition to optimizing instrumental parameters, we replaced the pneumatic nebulizer with an ultrasonic one.

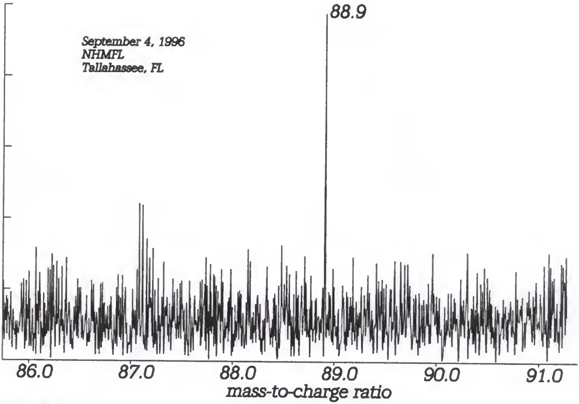

Figure 4-8
This is a mass spectrum of the first analyte ever observed with an ICP-FTICR system. The analyte was a 1,000 mg/L solution of yttrium and a pneumatic nebulizer was used.

Figure 4-9 is an ICP-FTICR broadband, single-scan spectrum of a 1 mg/L copper solution acquired with the NHMFL instrument. The mass resolving power ($m/\Delta m_{10\%V}$) was 6,800 (based on the $^{63}Cu^+$ peak). The isotope distribution was consistent with the accepted values for copper, indicating minimal mass discrimination by the wire ion guide, at least over narrow mass ranges. Based on natural abundances, the concentration of ^{63}Cu

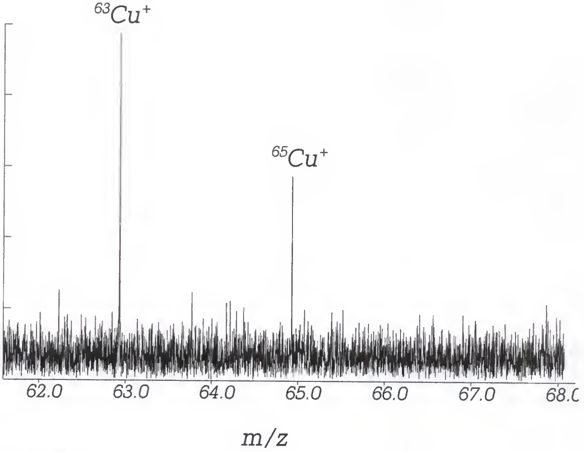

Figure 4-9
High resolution ($m/\Delta m_{10\%V}$ = 6,800) ICP-FTICR ms spectrum of a 1 mg/L copper solution obtained with the NHMFL instrument. Spectrum was obtained with one scan.

in this sample was *ca.* 690 ug/L, and the resulting $S/N \approx 8$. Although the analyzer cell pressure during these initial experiments was undesirably high by FTICR standards (*e.g.*, 10^{-8} torr), the mass resolving power for comparable solution concentrations demonstrated in Figure 4-9 rivaled that which could have been obtained with high resolution sector based ICP-MS instrumentation available at the time.

Figure 4-10 demonstrates the high resolving power capability of an FTICR instrument, even with analyzer pressures that are less than ideal for an FTICR experiment. The sample in this case was a 22 mg/L potassium solution. The spectrum in Figure 4-10a shows the region between m/z 40 and m/z 41; $^{41}K^+$ is resolved from $^{40}Ar^1H^+$. The theoretical mass resolving power ($m/\Delta m_\delta$) required to separate these two species is 4,890. The experimentally obtained mass resolving power ($m/\Delta m_{10\%V}$) was 10,000 as measured for the $^{40}Ar^1H^+$ peak. Figure 4-10b is an expanded view of the m/z 41 region, clearly showing both species baseline resolved.

These initial experiments served to highlight some important considerations for construction of an ICP-FTICR/MS instrument. For one, ions must be transported from the atmospheric pressure plasma to the high vacuum analyzer cell without large gaps in the ion optics.

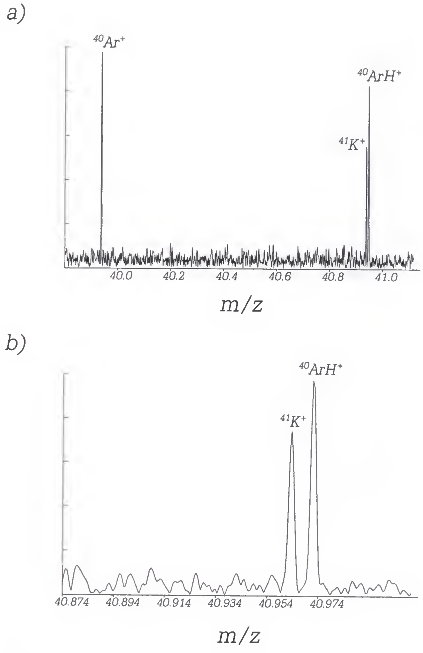

Figure 4-10

a) High-resolution ($m/\Delta m_{10\%V}$ = 10,000) ICP-FTICR MS broadband spectrum of a 22 mg/L potassium solution obtained with the NHMFL instrument showing separation of two species with the same nominal mass.

b) Expanded view mass region around m/z 41 showing baseline resolution of $^{41}K^+$ and $^{40}Ar^1H^+$.

As stated earlier, no analyte ions were observed with the UF instrument, most likely because the sampled ion beam was disrupted severely while traversing the large distance (*ca.* 15 cm) from the extractor lens (Label D in Figure 3-8) to the source-to-cell ion transfer optics at a pressure of 1×10^{-4} torr. This problem was lessened with the NHMFL instrument by shortening the distance between the extractor lens and wire ion guide (source-to-cell ion transfer device) to only *ca.* 5 cm.

Additionally, the spectra obtained with the UF instrument had a substantially lower noise background than those obtained with the NHMFL instrument (see Figure 4-11). The data station electronics of the UF instrument possessed much more extensive shielding. When the detection electronics are adequately shielded, the very small image currents measured in an FTICR experiment are not overwhelmed by the RF signal emanating from the ICP load coil, as critics suggested would be the case. Compared to that obtained at the NHMFL, the low noise background in the spectra acquired with the UF instrument highlights the importance of shielding the data station electronics from stray RF signals in ICP-FTICR.

Finally, experiments with both instruments confirmed that a minimum of four stages of differential pumping would be required to fully realize the ultrahigh resolving power benefits of ICP-FTICR MS.

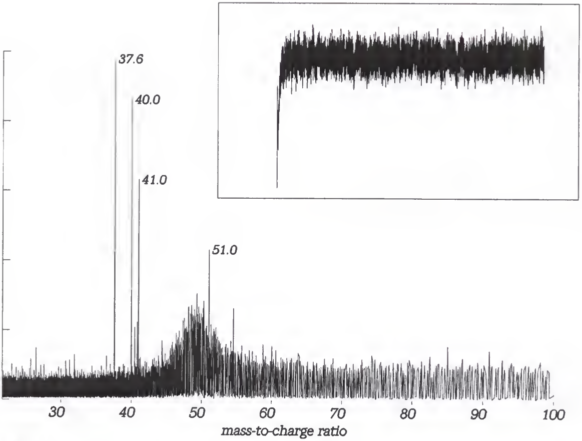

Figure 4-11
Argon spectrum acquired with the NHMFL instrument. The high noise background is attributed to the unshielded data station. The inset is the time domain spectrum which shows a large DC offset, an undesirable characteristic that results in higher noise across the entire bandwidth (*i.e.*, white noise).

Conclusions

Ions sampled from a high temperature ICP operating at atmospheric pressure were detected by FTICR MS. Spectra were obtained with resolving power that was sufficient to separate some spectral interferences that could not be separated with conventional ICP-MS instrumentation. At the analyte concentrations used in this study, the potential dynamic range problems presented by an overabundance of argon ions relative to analyte ions were not as severe as many would have expected. Furthermore, the dynamic range of an ICP-FTICR instrument can be extended by selective ejection of unwanted ions. These initial experiments also demonstrated the importance of thorough RF shielding of the data station electronics in ICP-FTICR MS experiments.

For samples with comparable solution concentrations, the mass resolving power obtained for analyte ions with the NHMFL instrument rivaled that which was obtainable with the best magnetic/electric sector based ICP-MS instruments. In conjunction with typical FTICR performance characteristics, the work presented here indicated to us that with future improvements (*i.e.* more efficient ion transfer, additional differential pumping, and better RF shielding), ICP-FTICR MS instrumentation would be capable of yielding even better mass resolving power with a simultaneous increase in sensitivity. An advanced ICP-FTICR source that was designed based on the results obtained in this work is presented in the next chapter. An account of this work was published in the literature.[116]

CHAPTER 5
DESIGN AND CONSTRUCTION OF AN OCTOPOLE BASED ICP-FTICR SOURCE

Introduction

The results obtained with previous ICP-FTICR source designs clearly indicated that an entirely new source would have to be constructed if we were going to demonstrate the full potential of the ICP-FTICR technique. The essential characteristics of this new source were well defined: in addition to incorporating good differential pumping, this source would also have to be capable of transmitting with high efficiency ions with a range of m/z values and kinetic energies.

Ion transmission through a device is usually accomplished via a series of electrostatic lenses, or alternatively an rf-only multipole device such as a quadrupole, hexapole, or octopole. We chose to incorporate an rf-octopole for a number of reasons. Since their inception,[117] octopoles have been used extensively for ion transmission by those interested in ion molecule reactions.[118,119] Additionally, they have been well-characterized in the literature. Unlike many publications regarding the subject that are highly mathematical in nature, and therefore of little use experimentally, this author found a work by Gerlich to be lucid and extremely useful from a design point of view.[120] It is known that rf-only octopoles can be operated as a high pass filter at a given frequency by increasing the peak-to-peak voltage of their drive frequency (see previous reference). This feature would be extremely useful in an ICP-FTICR experiment. For instance, the dynamic range of an ICP-FTICR instrument is comparatively limited. Although we have demonstrated that an overabundance of argon ions does not pose an insurmountable problem in an ICP-FTICR instrument, an octopole as part of the ion transmission optics could be used to prevent argon ions from entering the FTICR analyzer cell, thereby helping to increase the dynamic range of the technique. Of course, this removal could not be used if it were desired to determine ions with masses equal to or less than that of argon.

Design Considerations

The primary constraint in the design of this source was imposed by the space inside the source housing of the UF instrument, which was described previously. The source was to be designed to minimize the distance between where the ions are sampled and the entrance to the external ion transfer optics of the UF instrument, while simultaneously incorporating an extra stage of differential pumping. The source would also have to incorporate electrical feed-throughs for the connections that supply the rf to the octopole.

The aluminum source block shown in Figure 5-1 was designed first, and the rest of the components were designed around it. The large cutouts in the front of the source-block pictured in Figure 5-1 were to ensure adequate pumping of the extractor of the PlasmaQuad interface by a turbo-drag pump attached to the right hand side of the block, as it is shown in Figure 5-1. A turbo-drag pump was chosen to pump this region because of its very high pumping speeds for the magnitude of pressure that would be

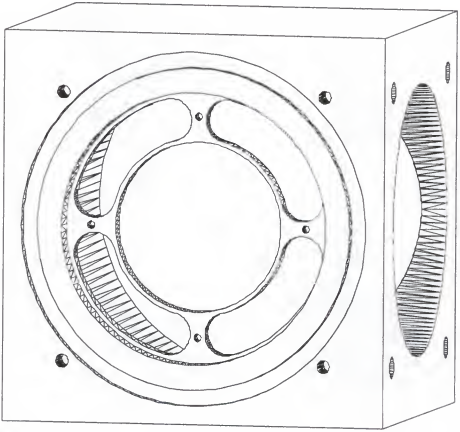

Figure 5-1
Aluminum source-block for the latest ICP-FTICR source. The PlasmaQuad interface attaches to the front, and the hole on the right hand side was designed to accommodate an ISO-100 flange.

present in this region. With the source-block designed, the remainder of the source was completed as shown in Figure 5-2.

After the source shown in Figure 5-2 was designed, it was attached to the external source FTICR system in Professor Eyler's laboratory, which was equipped with turbo-pumps, to test the differential pumping ability of the source.

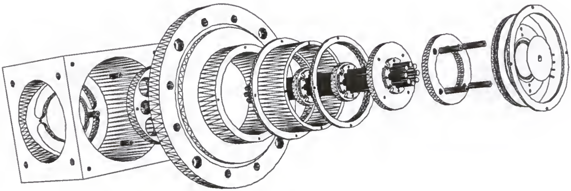

Figure 5-2
Exploded view of the ICP-FTICR source incorporating an octopole for increased ion transmission efficiency, along with an extra stage of differential pumping for more satisfactory pressure in the analyzer region of the FTICR. Note the removable conductance limit at the far right.

The differential pumping ability of the source was excellent by FTICR standards as shown in Figure 5-3, which is a plot of source and cell pressures as a function of conductance limit diameter. The conductance limit, which was electrically isolated from the source housing, is shown in Figure 5-2.

With the differential pumping of the source functioning as expected, the next task to be completed was the assembly of the electronics to operate the octopole. A schematic of this assembly is shown in Figure 5-4. As shown in Figure 5-4, the output from a frequency generator was sent to a power amplifier. Next, the amplified signal was sent to a center-tapped transformer with a 5:1 step-up ratio.

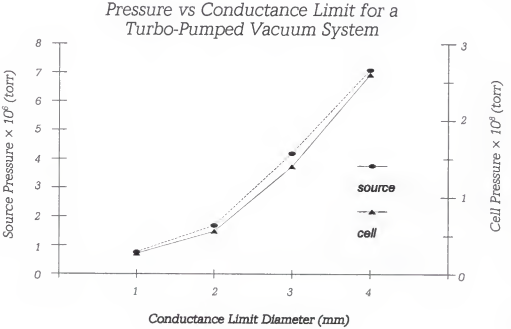

Figure 5-3
Differential pumping performance of ICP-FTICR source.

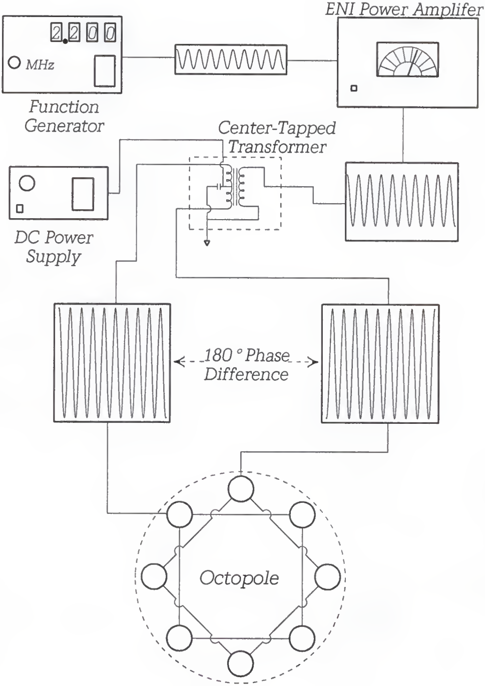

Figure 5-4
Wiring schematic of the electronics used to drive the octopole.

The center-tapped transformer split the signal into two equal components each 180° out of phase, a necessary requirement for the operation of any multipole device. The output from each secondary of the transformer was then sent to the octopole rods as shown. All electrical connections were coaxial-BNC. The function generator was a Hewlett Packard 8601A. The power amplifier was an ENI 2100L. The transformer was purchased from North Hills Signal Processing (Syosset, NY) by the NHMFL and loaned to us. It was further modified by our electronics shop as shown in Figure 5-4 with a capacitor-to-ground connection. This modification allowed a DC power supply to be used to apply a bias to the rods. The DC power supply shown in Figure 5-4 was a Kepco ATE-25.

The source was attached to the external vacuum source FTICR instrument described in Figure 4-3, which was now equipped with a 4.7T shielded magnet. We determined that accumulated-trapping was required to trap ions from this source.

Results and Discussion

The plot shown in Figure 5-5 is of copper signal as a function of the pulsed-valve duration used for accumulated trapping. We believe that the oscillatory nature of the signal at the end was due to variability induced by the high analyzer pressures in the FTICR cell that resulted from the long pulsed-valve durations. For all remaining experiments, a pulsed valve

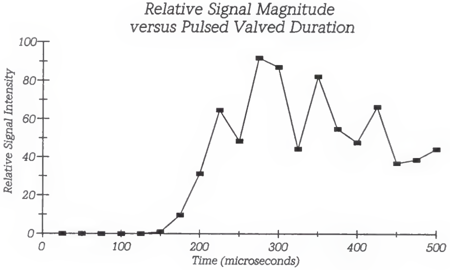

Figure 5-5
Normalized Copper Signal as a Function of Pulsed Valved Duration.

duration of 290 μs was used. Both argon and carbon dioxide were evaluated as cooling gases. Carbon dioxide was used because it could be pumped more efficiently by the cryopumps.

Figure 5-6 is an ICP-FT ICR spectrum of a 1.0 mg/L copper solution. As is apparent in this spectrum, the demonstrated resolving power and signal-to-noise with this octopole based source were much better than that obtained with previous designs.

The spectrum shown in Figure 5-6 was obtained before we optimized the operating conditions of the octopole. To determine the best parameters, we measured the relative transmission of a copper signal as a function of octopole drive frequency and applied rf power. The results are summarized in Figure 5-7.

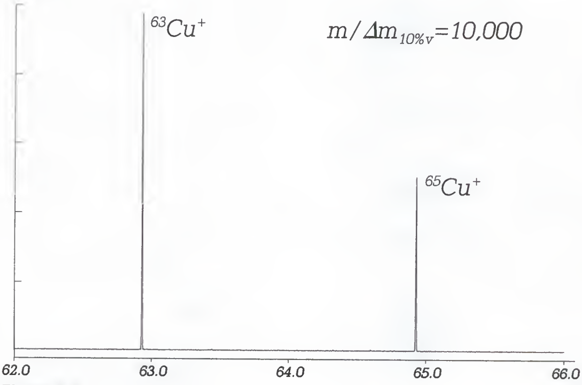

Figure 5-6
ICP-FTICR spectrum of a copper solution acquired with the newly designed octopole based source. Note the much improved signal-to-noise compared to previous spectra.

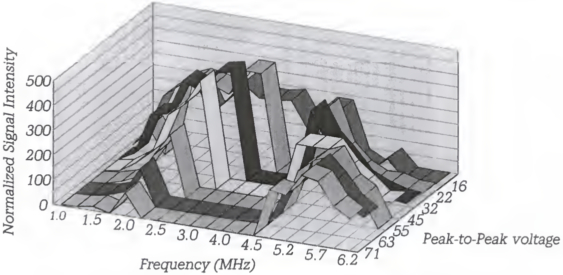

Figure 5-7
Normalized copper signal as a function of rf power and frequency.

In Figure 5-7 the valley in the middle of the plot is not due to a non–ideal region of transmission space, but rather to the impedance of the device being so large at these frequencies that the power amplifier was unable to produce voltages that were sufficient to drive the octopole.

Unfortunately, as is obvious from the plot, the ideal transmission of the octopole lies in this region. For the remainder of the experiments, a drive frequency of 2.5 MHz was used at an rf power that corresponded to 32 V_{pp} with this device.

The spectrum shown in Figure 5–8 demonstrates the potential for ultra–high resolving power of this source. Although the spectrum shown in Figure 4–10 was acquired with a system equipped with a magnet that has the potential for resolving powers that are a factor of two greater (7.0 T vs. 4.7

T), the resolving power and sensitivity demonstrated in the spectrum in Figure 5-8 are substantially better because of improved differential pumping and increased ion transmission. The combination of sensitivity and resolving power shown in this spectrum has never been demonstrated with any preexisting ICP-MS instrumentation as of the writing of this dissertation.

To determine the extent of mass discrimination of the octopole, we prepared a series of three solutions each containing 150 μg/L of copper and thallium. These two species were chosen because they have distinct isotopic patterns, they are representative of the mass range studied in elemental mass spectrometry, and no memory effects were observed for them. The solutions were prepared with a Gilson micropipet with disposable tips. The calibration of the pipet was verified by measuring the mass of ultra-pure deionized water delivered five times with different tips. The variation was small ($\sigma=\pm1$ μl). The signals from the three solutions showed a relative average deviation of ±10%. Figure 5-9 summarizes the results of this study. Figure 5-9 shows that the ICP-FTICR instrument with the octopole device does not mass discriminate to an appreciable degree. This figure also shows the effect that sample flow rate to the nebulizer (as it is depicted in Figure 3-2) has on the signal.

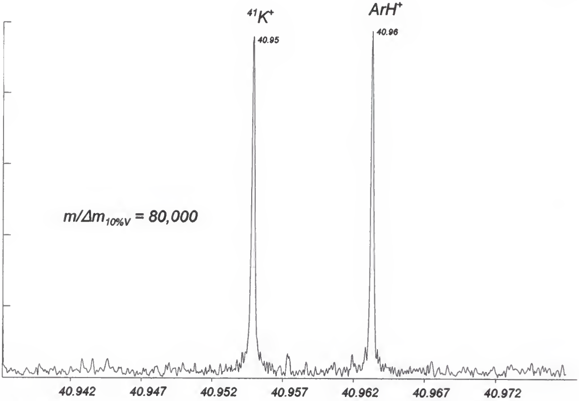

Figure 5-8
ICP–FTICR spectrum showing good sensitivity and complete baseline separation of two species with the same nominal mass. The concentration of $^{41}K^+$ in this spectrum was 400 μg/L. Compare to Figure 4–10

There are prominent peaks from rubidium, silver, and to a lesser extent, cesium in the spectra shown in Figure 5–9a and b. These were due to severe memory effects caused by deposits on the sampler and skimmer. We noticed the same effect for rubidium in the experiments at the NHMFL. The only way these memory effects could be eliminated was by removing the sampler and skimmer from the interface and polishing them. Copper and thallium exhibited no memory effects whatsoever as evidenced by Figure

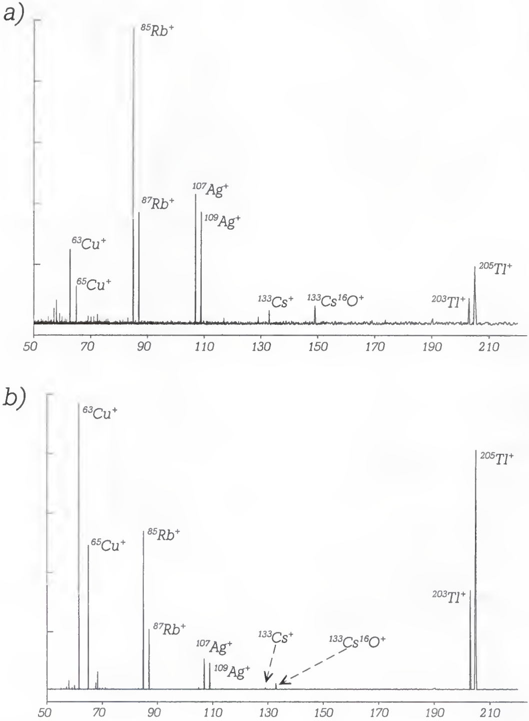

Figure 5-9
ICP–FTICR spectra acquired of a solution containing 150 μg/L each of copper and thallium.; a) pump flow rate = 0.25 mL/min; b) pump flow rate=5.0 mL/min

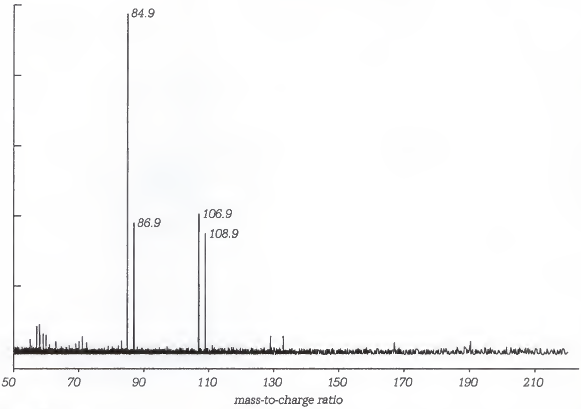

Figure 5-10
ICP–FTICR spectrum acquired with the ultrasonic nebulizer's transducer turned off.

5–10, which was obtained under the exact same conditions as Figures 5–9a and b, with the exception that the ultrasonic nebulizer was turned off.

One consequence that we had not anticipated was that side-kick trapping could not be used with this source. Accumulated trapping reduced the duty cycle to an appreciable degree, but not unbearably. The spectra shown in Figure 5–9, which possess a wide mass range by elemental standards, were acquired in 1.5 minutes.

Conclusions

This work has proven that an ICP–FTICR instrument is capable of producing spectra simultaneously with high mass resolving power and good sensitivity. The principal difficulties with previous designs, namely differential pumping, ion transmission, and rf shielding have been surmounted. Additionally, we ascertained that side–kick trapping was ineffective with this source design, but accumulated trapping worked well.

Based on the data obtained in these experiments, we estimate that with minor improvements, an ICP–FTICR instrument should be capable of detection limits in the low parts–per–trillion range with resolving powers of at least 10,000.

There are several features of the existing source that should be improved. Signal stability would be greatly improved by the addition of a mass flow controller. A torch translator that allows safe, precise positioning of the torch while the rf is activated would make signal optimization easier.

The plasma pinch that is characteristic of this source could be mitigated or eliminated altogether by connecting the ground side of the load coil to the sampler. Such a connection makes the plasma more difficult to ignite, but consequently more stable.

Finally, addition of a variable capacitor to the octopole drive circuitry would allow one to tune the circuit. This tuning would allow the octopole to be operated at an optimum frequency by selectively reducing the impedance. The best location for this capacitor would most likely be between the output of the function generator and the input of the center-tapped transformer.

With regard to future experiments, an even more detailed interference study should be conducted, and once an important species is found with a problematic interference, studies should be conducted to see if the existing instrumentation has the appropriate combination of sensitivity, dynamic range, and resolving power to distinguish the interference.

The work presented in this dissertation only hints at the potential of an ICP-FTICR instrument. The future work discussed in this section is limited to development of the ICP source itself; however, other developments in FTICR such as faster digitizers and larger capacity analyzer cells will complement this work nicely.

GLOSSARY

A/D converter: *See analog-to-digital converter*

accumulated trapping: FTICR trapping mechanism that results in increased trapping efficiency; externally created ions injected with a high kinetic energy are cooled by collisions with pulsed gas.

aerosol gas: In ICP-MS analyses, the gas that carries the sample in aerosol form through the center of the torch to the plasma; also referred to as the center gas.

aliasing: Observation of a signal of falsely low frequency due to digital sampling of the signal at a rate less than that specified by the Nyquist theorem.

analog signal: Signal comprised of a continuously-variable, physically measurable quantity.

analog-to-digital converter: Device that converts an analog signal into a digital signal.

analyzer cell: In FTICR MS, the device located in the center of the magnet where measurement of the image current signal occurs.

angular cyclotron frequency: $\omega_c = 2\pi\nu_c$ *(see cyclotron frequency)*

apodization: Multiplication of a time domain signal by a weighting function to minimize side-lobes or peak-tailing in the corresponding frequency domain signal. Depending upon the function, apodization can be used to improve S/N, or increase resolution, but never both simultaneously.

arbitrary waveform generator (AWG): Device used to produce ion excitation with results similar to that of SWIFT excitation. A series of frequencies and corresponding amplitudes are specified by the user and downloaded to the generator. The generator sums the time domain representations of the frequencies to create a final "arbitrary" time domain waveform that is the superposition of all the individual waveforms. Note that no inverse Fourier transform is performed.

auxiliary gas: In ICP-MS, the gas flow that sustains the plasma; also referred to as support gas.

bake-out: Process for quickly reducing the base pressure of a vacuum system by heating the walls for an extended period (e.g., 200° C for several hours). During the heating, gases that have been adsorbed by the metallic walls of the vacuum system are liberated.

bandwidth: The difference between the highest and lowest observed frequencies in a signal measurement.

base peak: The most intense peak in a mass spectrum.

beat pattern: In FTICR, the regularly spaced patterns of alternating constructive and destructive interference observed in time domain spectra. They are observed only when the detection event is sufficiently long and the spectrum consists of a few species that are similar in mass.

bit: In terms of digital storage, the smallest unit of information stored, usually represented as a 0 or 1.

broadband: Of, relating to, or having a wide range of frequencies (e.g., in FTICR, observable frequencies range from 10 kHz to 10 MHz, depending upon m/z and magnetic field strength).

CAD: *See collisionally activated dissociation.*

capacitive reactance: Reactance in a circuit due to capacitive elements. Effect becomes less pronounced as frequency is increased.

center-tapped transformer: Type of transformer with one primary winding and two secondary windings, each capacitively coupled to a common ground, thereby allowing the secondaries to be "floated" with respect to ground, but not each other. Useful for driving a multipole device since the current (and voltage) in the secondaries are 180° out of phase with each other.

chemical ionization (CI): Type of ionization whereby a volatile sample is introduced into source region where the partial pressure of a reactant gas (e.g., methane) is substantially higher. A filament is used to ionize the reactant gas by electron impact, wherein the reactant gas gently transfers a proton to the sample molecule, resulting in much less fragmentation of the sample than with an EI source.

chirp excitation: Excitation method in FTICR where a fast sweep generator is used to produce a wide range of frequencies (e.g., 10 kHz) over a short time (e.g., 1 ms)

CI: *See chemical ionization.*

CID: *See collisionally activated dissociation*

coherent ion motion: Motion of an ion packet in which all of the ions of the same m/z have the same nominal ICR orbital phase angle, radius, and orbital center.

collision gas: Gas that is introduced into either a trapped ion cell or multipole device, usually by a pulsed valve, for the purpose of interaction with ions.

collisional focusing: Introduction of a collision gas into a trapped ion cell or linear multipole at high pressure resulting in a focusing effect whereby the ions tend to aggregate about the center of the device.

collisionally activated dissociation: Heating of an ion by absorption of rf power followed by subsequent fragmentation upon impacting a collision gas molecule.

collisionally induced dissociation: *See collisionally activated dissociation.*

conductance limit: Limiting aperture in the form of either an open tubular capillary, or an opening in a thin metal plate for the purpose of restricting gas flow while simultaneously permitting the transmission ions.

cooling gas: 1) Gas introduced into an ion trap for the purpose of reducing the kinetic energy of the ions via collisions. *See collisional focusing.*

2) Outermost gas flow in an ICP torch that helps to prevent the torch from melting.

correlated excitation: Excitation mechanism that minimizes unintentional off-resonant excitation of ions of interest.

cryopump: Type of pump capable of ultra-high vacuum whereby the pumping action is induced by cooling a large surface area with liquid helium. Pumping speeds are widely disparate for different gases, with very high values (*e.g.*, 100-10,000 L/min) for N_2, H_2O, CO_2, *etc.*)

cubic cell: Symmetric FTICR analyzer cell possessing three mutually perpendicular axes.

cyclotron equation: $\nu = \frac{qB_0}{2\pi \cdot m}$; (all quantities in S.I. units)

cyclotron frequency: The frequency at which an ion in a magnetic field orbits as a result of the combined action of the Lorentz and centrifugal forces exerted on it.

cyclotron motion: Natural orbital motion of an ion in a magnetic field.

cyclotron phase angle: Angular displacement of an ion from an arbitrary reference point.

cylindrical analyzer cell: FTICR analyzer cell with cylindrical geometry.

D/A converter: *See digital-to-analog converter.*

DAC: *See digital-to-analog converter.*

dalton: Unit of mass (denoted Da) equivalent to 1/12 the mass of a ^{12}C atom.

Delrin: Brand name of a plastic noted for its excellent machining properties, particularly its ability to hold threads and maintain good tolerances (± 0.001") and very low cost. **Note**: Delrin is available in an almost unlimited range of sizes and shapes. Two major factors limit the range of Delrin's usefulness: it can be used in medium vacuum applications (*i.e.*, those requiring vacuum pressures no less than about 10^{-7} torr); and its maximum working temperature is 80° C, therefore it should not be used in applications where it will be subjected to heat. In applications where a part will be subjected to high thermal stress or is to be used in a high vacuum, a plastic such as PEEK or Teflon should be used.

detect event: The portion of an FTICR experiment where the image current in the detection electrodes is measured.

detection efficiency: In mass spectrometry, the ratio of the total number of ions detected with respect to the total number produced during the time required for acquisition of a spectrum.

Dewar: Originally, a flask used to store liquified gases that was constructed by evacuating the space in a double-walled container and coating the vacuum walls with a silvery, highly reflective material. Any device that is used to contain liquified gases is now commonly referred to as a Dewar. (Named after Scottish-born chemist Sir James Dewar).

DFT: *See discrete Fourier transform.*

differential detection: Detection method in FTICR where the resultant signal is measured as the difference between signals observed at the detection electrodes.

differential pumping: Arrangement whereby separately pumped regions of a vacuum system are joined by a conductance limit.

digital resolution: In FTICR, quantity equal to the observed signal bandwidth divided by the number of sampled data points, usually expressed as (Hz). **Note:** A smaller value for the digital resolution corresponds to a higher resolving power. For FTICR experiments, the spectral resolution is often limited by the digital resolution.

digital–to–analog converter: Device that converts an analog signal to a digital signal.

digitization rate: Number of samples acquired per unit time by the DAC, usually expressed as samples/sec or in units of frequency (Hz, kHz, MHz, *etc.*)

digitizer: *See digital–to–analog converter.*

digitizer frequency: *See digitization rate*.

discreet Fourier transform: Algorithm used with discrete, evenly spaced data to approximate the continuous Fourier transform.

drift cell: Type of analyzer cell employed in the early ICR mass spectrometers.

duty cycle: A measure of the time–efficiency of an analytical technique. It could be evaluated as the number of measurements over a specified range performed by the technique per unit time.

dynamic range: The difference between the largest and smallest sample concentrations that will produce undistorted signals.

EI: *See electron impact ionization.*

electron impact ionization (EI): Bombardment of a sample with high energy electrons (*e.g.*, 70 eV) to produce ionization via loss of electrons for positive ion mode, or acquisition of electrons for positive ion mode.

electrospray ionization (ESI): Remarkably successful method for production of ions by application of a high voltage (*e.g.*, 3–5 kV) to a solution containing an analyte with functional groups capable of sustaining a charge. Used primarily for biomolecules, although has been used with other sample types.

ESI: *See electrospray ionization*.

excitation: Application of rf power to an ion that increases its kinetic energy.

excite event: In FTICR, the portion of the experimental sequence that excites the ions either for isolation, ion-molecule reactions, or detection.

external injection ion optics: System of electrodes for external ion injection.

external ion injection: Process of guiding externally produced ions to the analyzer cell of an FTICR mass spectrometer.

external ionization: Production of ions outside the high magnetic field gradient of an FTICR mass spectrometer.

external source: FTICR instrument with an external ionization source. External sources usually incorporate several stages of differential pumping.

extractor lens: Electrode used to "pull" ions out of an ion source.

Fassel torch: Most common torch design used with ICPs; consists of three concentric quartz tubes accommodating an outer cooling gas flow, inner support gas flow, and central aerosol gas flow respectively.

fast Fourier transform: Remarkable DFT algorithm published by Tukey and Cooley in 1965 that reduces (compared with the direct DFT) the number of complex multiplications from N^2 to $\frac{1}{2}N \cdot \log_2(N)$ and complex addition/subtractions from $N(N-1)$ to $N \cdot \log_2(N)$ for data sets where N is an integral power of 2 (*i.e.*, $N = 2^n$, where n = 1, 2, 3,...). Based on multiplication count alone, a computer requiring 1 minute to compute a FFT for 32,768 (2^{15}) data points would require 4369 minutes to evaluate the conventional DFT for the same data set.

Fellgett advantage: *See multiplex advantage*.

FFT: *See fast Fourier transform*

Fourier analysis: Branch of mathematics where periodic functions are approximated by Fourier series.

Fourier series: An infinite series whose terms consist of constants multiplied by simple periodic functions that can approximate a wide range of functions if the series converges.

Fourier transform: Procedure based on Fourier analysis used to represent a continuous time function, f(t), as a continuous function of frequency, F(ω).

Fourier transform ion cyclotron resonance MS: Special type of ICR MS where the detected image current from an ensemble of ions of possessing a wide or narrow range of m/z values is collected simultaneously and subsequently Fourier transformed, resulting in a spectrum consisting of amplitude versus frequency. Upon processing via the cyclotron equation, the frequency spectrum is converted to a mass spectrum.

free ion decay: Decrease in kinetic energy of an ion due to frictional damping resulting in a transient with a characteristic exponential decay. As the kinetic energy of the ion decreases, its cyclotron radius decreases. As the distance between the ion and the detect electrode decreases, the induced image current also decreases.

frequency domain spectrum: Obtained upon application of the Fourier transform to the transient.

frequency generator: Device capable of producing (usually a variety of) waveforms (e.g., sinusoidal, triangular, sawtooth, square-wave, *etc*.) with varying amplitude (usually 0–10 V_{pp})

frequency shift: Undesirable effect observed in FTICR with a number of possible causes that has deleterious effects on mass resolution/mass accuracy and quantitation.

frictional damping: Decrease in kinetic energy of an ion via collisions with neutral molecules.

FTICR MS: *See Fourier transform ion cyclotron resonance MS*.

gate-valve: Device used to isolate portions of a vacuum chamber. Particularly useful in differentially pumped vacuum systems where it is desired to vent the low vacuum portion of the system while maintaining the ultra-high vacuum in the remainder of the system, thereby resulting in minimal down-time.

gauss: CGS unit of magnetic flux density (magnetic induction), equivalent to 1 maxwell·cm^{-2}

harmonic frequency: Frequency that is a whole number multiple of a "fundamental" frequency; for example, if the fundamental frequency is denoted by ω_0, then the harmonic frequencies would occur at $n \cdot \omega_0$, where n = 2,3,4,....

heterodyne: Mixing an observed signal with a reference signal to decrease the bandwidth.

high resolution MS: Mass spectrometry capable of producing spectra with $m/\Delta m$ in the range 10,000–100,000.

homogeneous line broadening: In FTICR, results from either loss of phase coherence of the ion ensemble, or a decrease in the signal amplitude as a result of ion-neutral collisions that serve to decrease the cyclotron radius. See inhomogeneous line broadening.

ICP–MS: *See inductively coupled plasma MS*.

ICP–FTICR MS: Inductively coupled plasma Fourier transform ion cyclotron resonance mass spectrometry.

ICR: *See ion cyclotron resonance*

ICR MS: Type of mass spectrometry based on the principle of ion cyclotron resonance.

ICR orbital phase: The angular position of an ion in an FTICR analyzer cell measured with respect to an arbitrary reference point.

image current: The current induced in a set of detection electrodes as ions pass near them.

impedance: A measure of the total opposition (capacitive, inductive and resistive) to current flow in a circuit impulse excitation: Application of a high amplitude, narrow width "DC" pulse to the excite plates of an FTICR analyzer cell. Noted for its simplicity, ability to excite a wide mass range simultaneously and more accurate isotope ratios, but difficulty in exciting ions below a critical m/z.

inductive reactance: Reactance that arises from inductive elements in an AC circuit. Becomes more pronounced as frequency increases.

inductively coupled plasma: High temperature (e.g., 6 000–8 000 K excitation temperature) atmospheric pressure discharge sustained by application of high frequency (e.g., 27 or 40 MHz) rf to a load coil encircling the end of a quartz torch with an inert gas (typically argon) flowing through it.

Infinity cell: Trademark FTICR cell designed to minimize z–axis ejection via a series of segmented trapping electrodes capacitively coupled to the excite plates.

inhomogeneous line broadening: In FTICR, arises when different resonance frequencies are observed for identical ions. Could arise from an inhomogeneous magnetic field, or by deviation from the ideal quadrupolar electrostatic trapping potential in the ion trap.

injection time: Time spent allowing ions from an external source to be transferred to the analyzer region of an FTICR instrument.

internal ionization: Ionization that occurs within the high magnetic field gradient of an FTICR MS.

inverse Fourier transform: Fourier analysis procedure used to represent a continuous function of frequency, $F(\omega)$, as a continuous function of time, $f(t)$. It is almost computationally identical to the Fourier transform.

ion cyclotron orbital frequency (ν_c):

ion cyclotron resonance: Orbital motion experienced by an ion in a magnetic field.

ion source: Primary means or region of the mass spectrometer where ions are produced; ions can be produced (either intentionally or unintentionally) in other parts of the mass spectrometer through processes such as photoionization, secondary discharge, CAD, *etc*.

ionization: Process whereby a neutral atom or molecule acquires a net charge.

ionization energy: The energy required to remove completely an electron from its neutral atom.

ionization potential: Used interchangeably with *ionization energy*. The term *ionization potential* is probably more widely used than ionization energy, but the latter is a more accurate descriptor of the quantity being measured.

isobaric: Term used to describe two different atoms (*i.e.,* different numbers of protons) with the same nominal mass.

isobaric ion interference: Type of *spectral interference* in elemental mass spectrometry that arises when background ions have the same nominal mass (m/z) as an analyte ion.

Johnson noise: *See thermal noise*.

leak valve: Used to maintain a constant partial pressure of gas in a vacuum pumped region.

load coil: Electrode used in ICP-MS to couple the rf power with the inert gas.

Lorentz force: The force experienced by an ion in combined electric and magnetic fields.

$$\vec{F} = q\vec{E} + q\vec{v} \times \vec{B}$$

m/z: A dimensionless quantity representing the mass of an ion (m) measured in Da, divided by the **number** (*i.e.,* not the charge itself) of fundamental charges (z) possessed by the ion, where the fundamental charge is that of an electron, $|e|$. It should be apparent from this definition that *m/z* **is not** the mass-to-charge (m/q, where $q = z \cdot e$) ratio of an ion.

machinable: Capable of being cut, tapped & threaded, formed, or otherwise modified with items normally found in most machine shops (*e.g.*, lathe, milling machine, drill press, *etc.*).

Macor: Brand name of a machinable ceramic manufactured by Corning. **Note:** Macor has a number of distinct advantages: it is manufactured in a large variety of sizes and shapes (*e.g.*, disks, rods, tubes, sheets, *etc.*); it is very nonporous, making it an excellent choice for use in high vacuum applications; and it has a very high maximum working temperature (*e.g.*, >1000° C). It can be tapped and threaded and machined to high tolerances, but it is very fragile. The major factors limiting Macor's usefulness are its fragility and relatively high cost. Macor should not be used in applications where it will be subjected to high mechanical stress, or when other materials will suffice. See *Delrin, PEEK,* and *Teflon*.

magnetic field homogeneity: The deviation of magnetic flux in a given volume of space. Typical values for super conducting magnets are on the order of 1 part in 10^5.

magnetic field strength: Quantity used to describe magnetic phenomena in terms of the forces exerted by their magnetic fields and/or degree of magnetization, often denoted **B** and measured in tesla. **Note**: Magnetic field strength has not been designated as an official SI unit, but some have chosen to derive it from base units as A/m. *See* **Note** at *magnetic flux density*.

magnetic flux: A measure of the total quantity of magnetism (*i.e.,* the total number of magnetic lines of force) passing through a specified area in a magnetic field. *See weber, tesla, magnetic flux density*.

magnetic flux density: (*Symbol* B or $\vec{\mathbf{B}}$) The amount of magnetic flux in a unit area taken perpendicular to the direction of the magnetic flux. **Note**: When discussing magnetic field strength, many people specify the magnetic flux density. Some confusion arises in part because there is no official SI unit for magnetic field strength, although some have chosen to derive it from base units as a scalar quantity with units of A/m.

magnetic mirror effect: Effect observed when ions pass through a rapidly changing magnetic field gradient, whereby the ions are deflected from their path of travel because of their tendency to follow the magnetic lines of force.

magnetron motion: Low frequency oscillation of ions in a Penning ion trap that arises as a consequence of the trapping field.

mass discrimination: For a mass spectrometer, variation in analytical sensitivity as a function of m/z.

mass resolution: The mass (actually, m/z) difference, Δm_x that exists between two adjacent peaks in a mass spectrum that are of equal size and shape (Gaussian, Lorentzian, or triangular) with a specified amount of overlap, where the subscript "x" denotes the overlap criterion (10% valley, Full Width at Half Height [FWHH], etc.). In the special case where $x=\delta$, the mass resolution is determined simply by the difference in masses for two given species. See **Note** for *mass resolving power* and *theoretical mass resolving power*

mass resolving power: The quantity, $m/\Delta m_x$, where Δm_x is the *mass resolution*. See **Note** for *theoretical mass resolving power and mass resolution*. ***Note***: Although the definition of mass resolution is contingent upon two adjacent, mass spectral peaks of equal size and shape, which is almost never the case experimentally, it is acceptable to calculate the *mass resolving power* or *mass resolution* from a single peak. An assumption is made about the peak shape, whereby the peak width at 5% height for a single peak would be approximately equivalent to the distance between the apexes of two peaks with a 10% valley between them (see figure below). This assumption is not unreasonable for most common peak shapes encountered in mass spectrometry. Therefore, the mass resolving power that is obtained by dividing the mass (m/z) value at the apex of a peak by the peak width at 5% of the peak height could be indicated as $m/\Delta m_{10\%V}$. (see figure below)

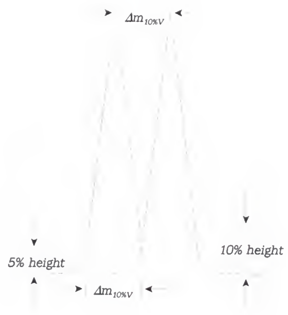

mass shift: *see frequency shift.*

matching box: Device used in ICP–MS to match the impedance of the rf generator with that of the plasma, thereby ensuring that most of the power from the generator is dissipated in the plasma, and not the generator.

matrix assisted laser desorption ionization: Method used primarily for biomolecules and polymers. Analyte is dissolved in a matrix which is subsequently impacted with photons from a laser. The matrix is selected based on its ability to absorb photons strongly at the wavelength of the laser.

maxwell: CGS unit of magnetic flux equal to 10^{-8} weber.

mechanical pump: Name given to pumps capable of attaining vacuum pressures as no lower than about 10^{-4} torr.

modulation: Variation of a property of an electromagnetic wave or signal (e.g., phase, frequency, or amplitude).

MS/MS: *see tandem MS.*

MS^n: A tandem MS experiment where n specifies the number of stages of MS performed.

multiplex advantage: Advantage in either time savings or improved S/N that results when a method is capable of acquiring many channels of data simultaneously, as opposed to a single channel at a time. An example is FTICR, which can acquire an entire spectrum in a few milliseconds, versus conventional single frequency ICR where typical acquisition times are of the order of 15-30 minutes.

multipole: Class of devices consisting of an even number of metal rods (poles) arranged such that adjacent rods are electrically isolated, but rods that are 180° opposed are electrically shorted. **Note**: For mass selection, quadrupoles are the best choice, but for ion transmission efficiency, octopoles (or even decapoles, 32-poles, *etc.*) work better. There is much contention regarding the use of hyperbolic rods versus cylindrical rods in quadrupole devices used as mass filters. However, most workers would agree that cylindrical rods work just as well as rods of hyperbolic cross section if the device is to be used solely for ion transport. Given that cylindrical rods are readily available at low cost, whereas rods of hyperbolic cross section are about a factor of 100-200 greater in price, cylindrical rods are used when mass selection is not necessary.

non-resonant ion: An ion that receives no rf power during an FTICR experiment.

Nyquist criterion: Specifies the *minimum* rate at which a periodic function must be digitized in order to avoid aliasing.

Nyquist frequency: For simple periodic functions, equal to 2ν, where ν is the highest frequency in the signal. **Note**: If the highest frequency to be observed is not the highest frequency in the sample, but still less than the Nyquist frequency, then a low pass filter must be used to avoid complication of the spectrum from aliased signals.

octopole: Type of multipole consisting of 8 rods. Used almost exclusively for high efficiency transport of ions. See **Note** at *multipole*.

open analyzer cell: Type of FTICR cell that does not contain traditional trapping electrodes such as plates or screens, resulting in an open geometry.

outer gas: *See cooling gas*.

Paul ion trap: Device that uses static and rf electric fields to trap ions. Forms the basis of quadrupole ion trap mass spectrometry.

peak coalescence: Observed in FTICR when number of ions exceeds trap capacity or when two ions are similar enough in mass that their cyclotron frequencies differ by only a few Hz or less, resulting in unresolved peaks in the mass spectrum.

peak tailing: Observed in FTICR MS when unapodized magnitude-mode spectra are acquired. Characterized by a narrow half-width, but a very broad base which can obscure minor constituents.

PEEK: Poly-ether-ether-ketone. Plastic noted for its excellent machining properties, suitability for use in high vacuum applications, and ability to withstand high thermal stress (e.g., maximum working temperature ≈ 800°). **Note**: PEEK combines many of the advantages of Delrin and Teflon. The major factor limiting PEEK's use is its very high cost. See *Delrin, Macor,* and *Teflon*.

Penning ionization: Form of ionization that is the result of neutral atoms or molecules in an excited state colliding with other species to form an ion.

Penning ion trap: Device that traps ions via the combined effects of a spatially homogeneous static magnetic field and three dimensional quadrupolar electrostatic trapping field directed along the magnetic field axis.

peristaltic pump: Pump designed to minimize contamination of a liquid sample by ensuring that the sample never comes in contact with any parts of the pump itself. A piece of polyethylene tubing is wrapped around a set of rollers on the pump and pressed against a curved surface. As the rollers are turned, liquid is drawn through the pump via peristaltic action.

pinch: Undesirable secondary discharge observed in ICP–MS that arises because of a potential difference between the load coil and sampler or skimmer. Results in decreased sensitivity for analyte, nickel contamination (from the sampler/skimmer) in the spectrum, and the presence of doubly charged species.

pneumatic nebulizer: Device used in ICP–MS to convert a liquid sample to an aerosol. Liquid sample delivered by a peristaltic pump to the nebulizer is combined with a gas and forced through a small orifice, resulting in a fine mist.

polyatomic ion interference: In ICP–MS, an ion formed either in the plasma or interface with the same nominal mass as an analyte ion. **Note**: some workers also choose to call polyatomic ion interferences *isobaric* ions. Given that the widely accepted definition of *isobaric* refers only to **atoms** of the same mass, and the fact that some methods of removing polyatomic ion interferences are incapable of removing isobaric ion interferences, this author feels that it is useful to classify the two types of interferences separately.

power amplifier: Device that increases the amplitude of an input signal over a given frequency range with a specified maximum level of distortion.

pressure broadening: Broadening of FTICR mass spectral peaks that results from a loss of spatial coherence of an ion ensemble due to pressure.

pulsed valve: Valve used to introduce varying amounts of gas into a vacuum system for brief periods. A TTL signal triggers a solenoid, which in turn opens the valve. The duration of the TTL controls the amount of time the solenoid is open, and hence, the amount of gas allowed into the system. For introduction of a gas into the high vacuum analyzer region of the FTICR instrument, TTL signals in the range of 30–500 μs are typically used.

QA: *See quadrupolar axialization.*

QEA: Quadrupolar excitation axialization, *see quadrupolar axialization.*

QIT: *See quadrupole ion trap.*

quadrature detection: Method of detection in FTICR where 4 plates are used instead of two, resulting in a $\sqrt{2}$ fold increase in S/N, but it is also instrumentally more difficult than traditional differential detection.

quadrupolar axialization: Method for "shrinking an ion cloud" in FTICR MS resulting in considerably enhanced remeasurement efficiency. QE is applied in the presence of a high pressure of collision gas (10^{-4} - 10^{-6} torr) introduced by a pulsed valve. In the absence of the QE, the ions would be lost from the cell at such high background pressure because their magnetron radii would increase rapidly. In the presence of the QE however, magnetron motion is interconverted to cyclotron motion, which is much more effectively damped by the collision gas, resulting in the return of the ions to the center of the trap.

quadrupolar excitation (QE): Method of excitation that interconverts magnetron motion to cyclotron motion by capacitively coupling the trapping electrodes with the excite electrodes.

quadrupole ion trap: *See Paul ion trap.*

quadrupole MS: Mass spectrometer that uses a quadrupole mass filter as the means of mass determination. See **Note** at *multipole*.

quench pulse: In FTICR, usually the first event in an event sequence; used to rid the analyzer cell of charged species that could contribute to space charge. Accomplished by placing voltages (~5 V) of equal magnitude and opposite polarity on each trapping electrode.

reactance: Opposition to the flow of current in an AC circuit due to elements other than resistors; usually expressed in units of ohms.

resolution: *See mass resolution.*

rf: radio-frequency.

rf burst excitation: See *impulse excitation.*

roughing pump: *See mechanical pump.*

sampler: In the sampling of ions in ICP-MS, the first element that a plasma impinges upon. It is usually made of nickel, with an orifice (typically, 0.5-1.0 mm diameter).

secondary discharge: In ICP-MS, occurs when a sufficient potential difference exists between two regions that causes electrons to flow from the region of higher potential to lower potential, resulting in a net current, usually visible as an arc.

sector MS: Type of mass spectrometer that sends ions through either a magnetic or electrostatic sector for mass determination.

side-kick: A feature of external source mass spectrometers manufactured by Bruker Daltonics (Billerica, MD) whereby externally injected ions are displaced from the central axis of the instrument by application of an electric field prior to entering the analyzer region. The moving ions interact with the electric and magnetic fields and experience a displacement (*i.e.,* side-kick) force.

sidebands: One of two frequencies, either above or below, a carrier frequency that result from modulation of the carrier.

side-lobes: The "wiggles" observed on each side of a center frequency, as shown below.

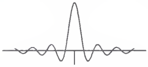

signal-to-noise ratio: A measure of the magnitude of an analytical signal relative to the collective magnitude of the signals due to noise in a physical measurement. **Note**: Although the idea of S/N is easy to understand, there is little agreement as to general approach that could be used to calculate it for all techniques.

single channel detection: In mass spectrometry, detection of a very narrow range of m/z at any given point in time. *See multiplex advantage.*

skimmer: The second element used in the sampling of ions from an ICP for ICP–MS. The skimmer is usually cone shaped and made of nickel with a hole through the center of it. It serves to sample as many ions as possible, while simultaneously rejecting as many neutrals as possible.

space charge: Name given to a number of undesirable effects observed in FTICR MS that result from too many ions (*i.e.*, charges) in a given volume of space. *See peak coalescence, frequency shift.*

spatial coherence: Term used in FTICR MS to describe ions of the same m/z that possess the same ICR orbital phase, radius, and orbital center.

spectral interference: Feature in a mass spectrum that impedes identification or quantitation of an analyte by causing an erroneously large signal to be measured for that analyte. *See isobaric and polyatomic ion interferences.*

stored waveform inverse Fourier transform excitation: FTICR excitation mechanism. A frequency domain power spectrum is specified by the user. Next, the inverse Fourier transform is applied to the spectrum to obtain a time domain representation, which is then used for excitation. A major advantage of SWIFT is true simultaneous excitation of all ions of a specified m/z.

super–conducting magnet ("super–con"): Magnet commonly used in FTICR because of the ability to attain high magnetic fields (commonly, up to 9.4 T), in addition to good field homogeneity, and field stability. Superconducting materials are fashioned into a solenoid and cooled to superconducting temperatures. The solenoid is then "energized" with an electric current, which induces the magnetic field. Current will circulate indefinitely with no resistive losses as long as the solenoid is kept below the critical temperature (*i.e.*, maximum superconducting temperature).

support gas: *See auxiliary gas.*

SWIFT: *See stored waveform inverse Fourier transform excitation.*

tandem MS: MS experiment where a first stage of MS is used to select a parent ion; the parent ion is then fragmented, and a second stage of MS is used to obtain a mass spectrum of the product ions.

tailored excitation waveforms: *See SWIFT.*

Teflon: Brand name for a polymer plastic manufactured by Dupont. **Note**: Teflon is capable of sustaining significantly higher working temperatures (*e.g.*, ~400° C) than Delrin. It is suitable for use in high vacuum applications (*i.e.*, $<10^{-8}$ torr) and is available in a wide variety of shapes and sizes. Teflon is machinable, but it cannot hold fine threads and cannot be machined to high tolerances like Delrin because it will "flow" like a viscous liquid when subjected to high mechanical stress. Furthermore, for comparably sized pieces, Teflon can be anywhere from 2–10 times more expensive than Delrin. Teflon should only be used in applications where it will not be subjected to mechanical stress and where high vacuum or high temperatures are present.

tesla: S.I. unit of magnetic flux density, equal to 1 Wb/m^2.

theoretical mass resolving power: $$\frac{m}{\Delta m_\delta} = \frac{m_1 + m_2}{2\,|m_1 - m_2|}$$

Note: *Theoretical mass resolving power* is useful for determining the relative difficulty in separating two peaks in a mass spectrum. The "masses" are actually m/z values, and the subscript "δ" indicates that the criterion used to determine Δm is simply the difference in mass between the two peaks. One should be careful to notice the subtle distinction between $\mathbf{\Delta m_\delta}$, a quantity that is independent of instrumental performance, and $\mathbf{\Delta m_x}$, a quantity that is determined by instrumental performance. It is important to realize that no peak shape assumptions are made in order to calculate the *theoretical mass resolving power*. Therefore, the choice of overlap criterion, *i.e.*, 10% valley, full width half height, etc. is the link between the *theoretical mass resolving power* and the experimentally measured *mass resolving power*. For an instrument to be capable of separating two particular ions, the instrument must possess a *mass resolving power* (over the range m + Δm) that is greater than the *theoretical mass resolving power* calculated for the ions in question.

thermal noise: Undesirable signals containing no useful information in electronic circuits that result from thermal agitation of electrons.

time domain spectrum: In FTICR, FTIR, and FTNMR for example, the directly obtained digitized spectrum consisting of amplitude as a function of time.

time of flight MS (TOF MS): MS technique were the m/z of the ions is determined by their flight time through a field free region. All ions are passed through the same potential difference, thereby imparting the same kinetic energy per unit of charge to each ion. Ions with small m/z arrive at the detector before heavier ions.

TOF: *See time of flight analyzer.*

transducer: Device for interconverting electrical energy and mechanical energy.

transient: The observed time domain spectrum in FTICR MS.

trapping oscillation: Periodic motion along the direction of the magnetic field vector experienced by ions in a Penning trap.

trapping potential: Voltage applied to the trapping electrodes of an FTICR analyzer cell to prevent the ions from escaping along the direction of the magnetic field lines.

TTL signal: Transistor–transistor logic. **Note**: TTL is a specification used by many electronic devices for communicating with other devices.

turbo-pump: Pump that uses a series of blades spinning at very high speed (~60,000 RPM) for the pumping action. These pumps operate under conditions and with specifications similar to cryopumps.

ultra-high resolution MS: MS producing spectra with $m/\Delta m$ in excess of 100,000.

ultrasonic nebulizer: Type of nebulizer used in ICP-MS experiments that utilizes a transducer consisting of a piezoelectric crystal to turn the liquid sample into an aerosol. As the liquid is deposited onto the face of the crystal, an rf signal is applied to the crystal causing it to vibrate at a high frequency, which subsequently converts the sample to a fine mist. These nebulizers are considered to improve mass transport and sensitivity by about a factor of 10 for most elements compared to pneumatic nebulizers.

weber: SI unit of magnetic flux, equal to 1 V·s.

white noise: Noise that is evenly distributed over a given bandwidth.

windowing: Original name for the multiplication of a time domain spectrum by a weighting function to minimize side-lobes. **Note**: When performed in the time domain, the process of multiplying the observed spectrum by a weighting function was called windowing originally. Alternatively, when the process was performed in the frequency domain, it was called apodization. Over the years, the term apodization has been used to describe weighting in both domains, and windowing is rarely used anymore.

word size: The number of bits used by a computer to represent a value for storage or processing. As the word size increases, the number of values that the computer can store decreases, but the dynamic range for each value increases.

z-axis motion: *See trapping oscillation.*

z-ejection: Ejection of ions along the z-axis in an FTICR experiment during excitation.

zero filling: Process of adding zeros to the end of a time domain spectrum. **Note**: If the number of data points to be transformed is not an integral power of two, zero filling can be used to make it so. In FTICR, zero filling is more commonly used to give a better representation of the frequency domain spectrum, but at the expense of increasing the estimation error of the FFT's representation of the continuous Fourier transform. As the number of zeros added increases, so does the FFT's estimation error of the continuous Fourier transform.

REFERENCES

(1) Montaser, A. *Inductively Coupled Plasma-Mass Spectrometry: From A to Z;* Wiley: New York, 1997.

(2) Jarvis, K. E; Gray, A. L.; Houk, R. S. *Handbook of Inductively Coupled Plasma Mass Spectrometry;* Blackie: Glasgow, 1992.

(3) Montaser, A.; Golightly, D. W. *Inductively Coupled Plasmas in Analytical Atomic Spectrometry;* VCH: New York, 1992.

(4) Houk, R. S.; Thompson, J. J. *Mass Spectrom. Rev.* **1988**, *7*, 425–461.

(5) Houk, R.S. *Anal. Chem.* **1986**, *58*, 97A–105A.

(6) Gray, A. L. In *Applications of ICP-MS,* Date, A. R.; Gray, A. L. Eds.; Blackie: Glasgow, 1989; p. 1–42.

(7) Evans, E. H.; Giglio, J. J. *J. Anal. Atomic Spectrom.* **1993**, *8*, 1–18.

(8) Sah, R. *N. Applied Spectrosc. Rev.* **1995**, *30*, 35–80.

(9) Reed, M. R.; Cairns, R. O.; Hutton, R. C.; Yuuichi, T. *J. Anal. Atomic Spectrom.* **1994**, *9*, 881–896.

(10) Tanner, S. D. *J. Anal. Atomic Spectrom.* **1995**, *10*, 905–921.

(11) Jakubowski, N.; Feldman, I; Stuewer, D. *Spectrochemica Acta* B **1994**, *47B,* 107–118.

(12) Alves, L. C.; Wiederin, D. R.; Houk, R. S. *Anal. Chem.* **1992**, *64*, 1164–1169.

(13) Clemons, P. S.; Minnich, M. G.; Houk, R. S. *Anal. Chem.* **1995**, *67*, 1929–1934.

(14) Goosens, J.; Moens, L.; Dams, R. J. *J. Anal. Atomic Spectrom.* **1993**, *8*, 921–926.

(15) Plantz, M. R.; Fritz, J. S.; Smith, F. G.; Houk, R. S. *Anal. Chem.* **1989**, *61*, 149-153.

(16) van Veen, E. H.; Bosch, S; de Loos-Vollebregt, M. T. C. *Spectrochemica Acta B* **1994**, *49B*, 1347-1361.

(17) Ketterer, M. E.; Biddle, D. A. *Anal. Chem.* **1992**, *64*, 1819-1823.

(18) Smith, F. G.; Wiederin, D. R.; Houk, R. S. *Anal. Chem.* **1991**, *63*, 1458-1462.

(19) Lam, J. W.; Horlick, G. *Spectrochemica Acta B* **1990**, *45*, 1313-1326.

(20) Rowan, J. T.; Houk, R. S. *Appl. Spectrosc.* **1989**, *43*, 976-980.

(21) Barinaga, C. J.; Koppenaal, D. W. *Rapid Comm. Mass Spectrom.* **1994**, *8*, 71-76.

(22) Koppenaal, D. W.; Barinaga, C. J.; Smith, M. R. *J. Analyt. Atomic Spectrom.* **1994**, *9*, 1053-1058.

(23) Barinaga, C. J.; Eiden, G. C.; Alexander, M.L.; Koppenaal, D. W. *Fresenius J. Anal. Chem.* **1996**, *355 (5/6)*, 487-493.

(24) Eiden, G. C.; Barinaga, C. J.; Koppenaal, D. W. *J. Analyt. Atomic Spectrom.* **1996**, *11*, 317-322.

(25) Bradshaw, N.; Hall, E. F.; Sanderson, N. E. *J. Analyt. Atomic Spectrom.* **1989**, *4*, 801-803.

(26) Morita, M.; Ito, H.; Linscheid, M.; Otsuka, K. *Anal. Chem.* **1994**, *66*, 1588-1590.

(27) Klinkenberg, H. *On the Use of Inductively Coupled Plasma Mass Spectrometry in Industrial Research* DSM Research, PO Box 18, 6160 MD, Geleen, The Netherlands, **1993**, p. 165.

(28) Ying, J. F.; Douglas D. J. *Rapid Comm. Mass Spectrom.* **1996**, *6*, 649–652.

(29) Goodner, K. L.; Milgram, K. E.; Watson, C. H.; Dejsupa, C.; Barshick, C. M.; Eyler, J. R. *J. Amer. Soc. Mass Spectrom.* **1996**, *7*, 923–929.

(30) Watson, C. H.; Barshick, C. M.; Wronka, J.; Laukien, F. H.; Eyler, J. R. *Anal. Chem.* **1996**, *68*, 573–575.

(31) Barshick, C. M.; Eyler, J. R. *J. Amer. Soc. Mass Spectrom.* **1993**, *4*, 387–392.

(32) Watson, C. H.; Wronka, J.; Laukien, F. H.; Barshick, C. M.; Eyler, J. R. *Anal. Chem.* **1993**, *65*, 2801–2804.

(33) Barshick, C. M.; Eyler, J. R. *J. Amer. Soc. Mass Spectrom.* **1992**, *3*, 122–127.

(34) Harrison, W. W. *J. Anal. Atomic Spectrom.* **1992**, *7*, 75–79.

(35) Harrison, W. W; Barshick, C. M.; Klingler, J. A.; Ratliff, P. H.; Mei, Y. *Anal. Chem.* **1990**, *62*, 943A–949A.

(36) Dunbar, R. C. *Mass Spectrom. Rev.* **1992**, *11*, 309–339.

(37) Marshall, A. G.; Grosshans, P. B. *Anal. Chem.* **1991**, *63*, 215A–229A.

(38) Knobeler, M.; Wanczek, K. P. "Detection of Harmonic Multiples of the Fundamental Frequency in Fourier Transform Ion Cyclotron Resonance MS" Presented at the 45th ASMS Conference on Mass Spectrometry and Allied Topics, **1997**, Palm Springs, CA.

(39) Nawrocki, J. P.; Wigger, M.; Watson, C. H.; Hayes, T. W.; Senko, M. W.; Benner, S. A.; Eyler, J. R. *Rapid Comm. Mass Spectrom.* **1996**, *10(14)*, 1860–1864.

(40) Guan, S.; Sik, H. S.; Marshall, A. G.; Wahl, K. C.; Wood, T.D.; Xiang, X. *Chem. Rev.* **1994**, *94*, 2161–2182.

(41) Speir, J. P.; Gorman, G. S.; Pitsenberger, C. C.; Turner, C. A.; Wang, P. P.; Amster, I. J. *Anal. Chem.* **1993**, *65*, 1746–1752.

(42) Valaskovic, G. A.; Kelleher, N. L.; McLafferty, F. W. *Science* **1996**, *273*, 1199–1202.

(43) Solouki, T.; Marto, J. A.; White, F. M; Guan, S.; Marshall, A. G. *Anal. Chem.* **1995**, *67*, 4139–4144.

(44) Bruce, J.E.; Cheng, X.; Bakhtiar, R; Wu, Q.; Hofstadler, S. A.; Anderson, G. A.; Smith, R. D. *J. Am. Chem. Soc.* **1994**, *116*, 7839–7847.

(45) Lawrence, E. O.; Livingston, M. S. *Phys. Rev.* **1932**, *40*, 19.

(46) Sommer, H.; Thomas, H. A.; Hipple, J. A. *Phys. Rev.* **1949**, *76*, 1877.

(47) Wobschall, D.; Graham, J. R.; Malone, D. P. *Phys. Rev.* **1963**, *131*, 1565.

(48) Baldeschwieler, J. D.; Randall, E. W. *Acc. Chem. Res.* **1963**, *63*, 81–110.

(49) Brauman, J. I.; Blair, L. K. *J. Am. Chem. Soc.* **1970**, *92*, 5986–5992.

(50) Llewellyn, P. *U. S. Patent* 3 505 517, **1970**.

(51) Low, M. J. D.; Freeman, S. K. *Anal. Chem.* **1967**, *39*, 93.

(52) McIver, R. T., Jr. *Rev. Sci. Instrum.* **1970**, *41*, 555.

(53) Marshall, A. G. *Acc. Chem. Res.* **1985**, *18*, 316–322.

(54) Comisarow, M. B.; Marshall, A. G. *Chem. Phys. Lett.* **1974**, *25*, 282–283.

(55) Cooley, J. W.; Tukey, J. W. *Mathematics of Computation* **1965**, *19*, 297–301.

(56) Garfield, E. *Current Contents* **1984**, *27*, 3–10.

(57) Yamashita, M.; Fenn, J. B. *J. Phys. Chem.* **1984**, *88*, 4451.

(58) Thomson, B. A.; Iribarne, J. V. *J. Chem. Phys.* **1979**, *71*, 4451.

(59) Little, D. P.; Chorush, R.A.; Speir, J. P.; Senko, M. W.; Kelleher, N. L.; McLafferty, F. W. *J. Am. Chem. Soc.* **1994**, *116*, 4893–4897.

(60) Little, D.; Thannhauser, T. W.; McLafferty, F. W. *Proc. Natl. Acad. Sci., U.S.A.* **1995**, *92*, 2318–2322.

(61) Hettich, R.; Buchanan, M. *J. Am. Soc. Mass Spectrom.* **1991**, *2*, 402–412.

(62) Gross, M. L.; Rempel, D. L. *Science* **1984**, *226*, 261.

(63) Johlman, C. L.; White, R. L.; Wilkins, C. L. *Mass Spec. Rev.* **1983**, *2*, 389.

(64) Asamoto, B. *Spectroscopy* **1986**, *3*, 38–45.

(65) Buchanan, M. V.; Hettich, R. L. *Anal. Chem.* **1993**, *65*, 245A–259A

(66) Kahr, M.S.; Wilkins, C. L. *J. Am. Soc. Mass Spectrom.* **1993**, *4*, 435.

(67) Dey, M.; Castoro, J. A.; Wilkins, C. L. *Anal. Chem.* **1995**, *67*, 1575–1579.

(68) Wu, J.; Fannin, S. T.; Franklin, M. A. *Anal. Chem.* **1995**, *67*, 3788–3392.

(69) Loh, S. Y.; McLafferty, F. W. *Anal. Chem.* **1991**, *63*, 546–550.

(70) Senko, M. W.; Beu, S. C.; McLafferty, F. W. *J. Am. Soc. Mass Spectrom.* **1995**, *6*, 52–56.

(71) Marshall, A. G. *Acc. Chem. Res.* **1996**, *7*, 307–315.

(72) Grover, R.; Decouzon, M.; Maria, P.; Gal, J. *European Mass Spectrom.* **1996**, *2*, 213–223.

(73) Sannes, K. A.; Brauman, J. I. *J. Phys. Chem.* **1996**, *100*, 7471–7479.

(74) Jiao, C. Q.; Ranatunga, D. R. A.; Freiser, B. S. *J. Phys. Chem.* **1996**, *100*, 4755–4759.

(75) Rodgers, M. T.; Campbell, S.; Marzluff, E. M.; Beauchamp, J.L. *Int. J. Mass Spectrom. Ion Proc.* **1995**, *148*, 1–23.

(76) Schindler, T.; Berg, C.; Niednerschatteburg, G.; Bondeybey, V. E. *J. Phys. Chem.* **1995**, *99*, 12434–12443.

(77) Mullen, S. L.; Marshall, A. G. *J. Am. Chem. Soc.* **1988**, *110*, 1766–1774.

(78) Kiplinger, J. P.; Tollens, F. R.; Marshall, A. G.; Kobayashi, T; Lagerwall, D. R.; Paquette, L. A.; Bartmess, J. E. *J. Am. Chem. Soc.* **1989**, *111*, 6914–6919.

(79) Stemmler, E. A.; Buchanan, M. V.; Hurst, G. B.; Hettich, R. L. *Anal. Chem.* **1995**, *67* 2924–2430

(80) Wu, Q. Y.; Vanorden, S.; Cheng, X. H.; Bakhtiar, R.; Smith, R. D. *Anal. Chem.* **1995**, *67*, 2948–2509.

(81) Li, Yu-Tsyr; Hsieh, Y-L; Henion, J. D.; Senko, M. W.; McLafferty, F. W.; Ganem, B. *J. Am. Chem. Soc.* **1993**, *115*, 8409–8413.

(82) Ross, C. W., III; Guan, S.; Grosshans, P. B.; Ricca, T. L.; Marshall, A. G. *J. Am. Chem. Soc.* **1993**, *115*, 7854–7861.

(83) Pfandler, P.; Bodenhausen, G.; Rapin, J.; Houriet, R.; Gaumann, T. *Chem. Phys. Lett.* **1987**, *138*, 195–200.

(84) Marshall, A. G. *J. Chem. Phys.* **1971**, *55*, 1343–1354.

(85) Comisarow, M. B.; Marshall, A. G. *J. Chem. Phys.* **1976**, *64*, 110–119.

(86) Marshall, A. G.; Comisarow, M. B.; Parisod, G. J. *J. Chem. Phys.* **1979**, *71*, 4434–4444.

(87) Wang, T.-C. L; Marshall, A. G. *Int. J. Mass Spectrom. Ion Proc.* **1986**, *68*, 287–301.

(88) Marshall, A. G. *Anal. Chem.* **1979**, *51*, 1710–1714.

(89) Wineland, D. J. *Science*, **1984**, *226*, 395–400.

(90) Marshall, A. G.; Grosshans, P. B. *Anal. Chem.* **1991**, *63*, 215A–228A.

(91) Chen, F. F. *Introduction to Plasma Physics and Controlled Fusion*; Plenum Press: New York, 1984.

(92) McIver, Jr., R. T. *Int. J. Mass Spectrom. Ion Proc.* **1990**, *98*, 35.

(93) Kofel, P.; Allemann, M.; Kellerhals, H.; Wancek, K. P. *Int. J. Mass Spectrom. Ion Proc.* **1985**, *65*, 97.

(94) Winger, B. E; Hofstadler, S. A.; Bruce, J. E.; Udseth, S. R.; Smith, R. D. *J. Am. Soc. Mass Spectrom.* **1993**, *4*, 566–577.

(95) Senko, M. W.; Hendrickson, C. L.; Pasa-Tolic, L; Marto, J. A. White, F. M.; Guan, S.; Marshall, A. G. *Rapid Comm. Mass Spectrom.* **1996**, *10*.

(96) Marto, J. A.; May, M. A. Marshall, A. G.; Limbach, P. A. *J. Am. Soc. Mass Spectrom.* **1995**, *6*, 936.

(97) Marshall, A. G.; Roe, D. C. *J. Chem. Phys.* **1980**, *73*, 1581–1590.

(98) Baldeschwieler, J. D.; Randall, E. W. *Acc. Chem. Res.* **1963**, *63*, 81–110.

(99) Grosshans, P. B.; Marshall, A. G. *Anal. Chem.* **1991**, *63*, 2057–2061.

(100) Heck, A. J. R.; de Koning, L. J.; Pinkse, F. A.; Nibbering, N. M. *Rapid Comm. Mass Spectrom.* **1991**, *5*, 406–414.

(101) Comisarow, M. B.; Marshall, A. G. *Chem. Phys. Lett.* **1974**, *26*, 489–490.

(102) Marshall, A. G.; Wang, T.-C. L.; Ricca, T. L. *J. Am. Chem. Soc.* **1985**, *107*, 7893–7897.

(103) Morrison, N. *Introduction to Fourier Analysis* John Wiley & Sons: New York; 1994; p. 45.

(104) Houk, R. S.; Fassel, V. A.; Flesch, G. D.; Svec, H. J.; Gray, A. L.; Taylor, C. E. *Anal. Chem.* **1980**, *52*, 2283–2289.

(105) Niu, H.; Houk, R. S. *Spectrochimica Acta B* **1996**, *51B*, 779–815.

(106) Scott, R. H.; Fassel, V. A.; Knisely, R. N.; Nixon, D. E. *Anal. Chem.* **1974**, *46*, 75–80.

(107) White, F. M; Marto, J.; Marshall, A. G. *Rapid Comm. Mass Spectrom.* **1996**, *10*, 1845–1849.

(108) Marto, J. A.; May, M. A.; Limbach; P. A.; Marshall, A. G. *J. Amer. Soc. Mass Spectrom.* **1995**, *6*, 936–946

(109) Senko, M. W.; Canterbury, J. D.; Guan, S.; Marshall, A. G. *Proc. of 43rd ASMS Conference on Mass Spectrometry and Allied Topics*, **1995**, p. 733, *Atlanta, GA.*

(110) Watson, C. H.; Goodner, K. L.; Eyler, J. R. *Proc. of 44th ASMS Conference on Mass Spectrometry and Allied Topics*, **1996**, p.1191, *Portland, OR.*

(111) Ferrige, A. G.; Lindon, J. C. *J. Magnetic Reson.* **1978**, *31*, 337–340.

(112) Eiden, G. C.; Barinaga, C. J.; Koppenaal, D. W. *Rapid Comm. Mass Spectrom.* **1997**, *11*, 37–42.

(113) Marshall, A. G.; Wang, T–C L.; Ricca, T. L. *J. Am. Chem. Soc.* **1985**, *107*, 7893–7897.

(114) Hanson, C. D.; Castro, M. E.; Kerley, E. L.; Russell, D. H. *Anal. Chem.*, **1990**, *62*, 1352–1355.

(115) Heck, A. J. R.; de Koning, L. J.; Pinkse, F. A.; Nibbering, N. M. *Rapid Comm. Mass Spectrom.*, **1991**, *5*, 406–414.

(116) Milgram, K. E.; White, F. M.; Goodner, K. L.; Watson, C. H.; Koppenaal, D. W.; Barinaga, C. J.; Smith, B. H.; Winefordner, J. D.; Marshall, A. G.; Houk, R. S.; Eyler, J. R. *Anal. Chem.* **1997**, *69*, 3714-3721.

(117) Teloy, E.; Gerlich, D. *Chem. Phys.* **1974**, *4*, 417.

(118) *Kinetics of Ion-Molecule Reactions*; Ausloos, P., Ed.; Plenum Press: New York, 1979.

(119) *Structure/Reactivity and Thermochemistry of Ions*; Ausloos, P.; Lias, S. G., Eds.; Reidel: Dordrect, 1987.

(120) Gerlich, D. in *State-Selected and State-to-State Ion Molecule Reaction Dynamics, Part 1: Experiment*; Ng, C. Y.; Baer, M., Eds.; John Wiley & Sons: New York, 1992, pp. 1–176.

BIOGRAPHICAL SKETCH

Kenneth "Eric" Milgram was born in Jacksonville, Florida on March 10, 1970. His childhood and teen years were spent in Winter Haven, a city in central Florida with an abundance of lakes.

During his time in Winter Haven, Eric had a varied work experience that included a furniture store, K-mart department store, and the popular tourist attractions Cypress Gardens and Walt Disney World.

Throughout his early years in school, Eric perceived his mathematics courses as dull and uninteresting. As ~~he~~ a, the? result he assumed that he was incapable of comprehending the subject, and so he decided that if he were to attend college, he would be an English major. However, his thinking changed dramatically during his sophomore year in high school, when, just as he was about to transfer out of his geometry class to a course in business math, he began to comprehend the abstract subject. Because of this newly discovered understanding, he took a greater interest in the remainder of his science and math courses. After graduating from Winter Haven High School in 1988, he attended Polk Community College, which is also located in Winter Haven, for one year. Next, he transferred to the University of Florida in Gainesville.

Because of the strong background that he received in high school and his predilection for the field, Eric decided to major in chemistry. During his first summer break from the University of Florida, Eric approached Dr. Harold Browning, an entomologist at the University of Florida's Citrus Research and Education Center in Lake Alfred, about working for the summer in his laboratory. Dr. Browning offered Eric a position, and sensing Eric's desire to learn more about instrumentation, he also arranged for Eric to work part-time for toxicologist Dr. Herbert Nigg. The combined experiences in both laboratories stimulated Eric's interest in applied research.

During his third year of undergraduate study, he inquired about a job posting seeking a chemist. Although he had little practical experience, Eric's enthusiasm and desire to learn was enough for Professor Donn Shilling to give him a job in his laboratory. Under Professor Shilling's direction, Eric developed methods for studying the relationships between herbicides and natural compounds in plants. Additionally, he acquired a strong background in analytical methods development. Convinced that he should attend graduate school, Eric applied to a number of graduate programs, but he decided that he would remain at the University of Florida because of its strong analytical chemistry program.

Eric chose Professor John Eyler and Graduate Research Professor James Winefordner as his co-research advisors. Under their guidance, Eric designed and constructed analytical instrumentation that has overcome some limitations with a common method of elemental analysis known as inductively coupled plasma mass spectrometry (ICP-MS). For example, there was no ICP-MS method that was capable of distinguishing relatively harmless uranium-238 from deadly plutonium-238. However, the U.S. Department of Energy's Pacific Northwest National Laboratory in Richland, Washington has expressed interest in Eric's research for this purpose. Eric earned his Ph.D. degree in December 1997.

Based on his research accomplishments, Eric was awarded a prestigious fellowship from the Oak Ridge Institute for Science and Education (ORISE). The fellowship is to be fulfilled in the toxicology group of the National Center for Environmental Health of the U.S. Centers for Disease Control and Prevention (CDC). In this job, Eric will develop methods to determine the levels of environmental toxins such as dioxins, polychlorbiphenyls, and polyaromatic hydrocarbons in human subjects. Additionally, he will also serve as a member of the CDC's Emergency Response team. Members of this team are constantly on alert for crises where people are exposed to environmental toxins. The goal of this team is to develop analysis methods for quickly determining the amount of toxins in human subjects. This information helps epidemiologists to measure exposure, and consequently, to prescribe appropriate treatment for exposed individuals.

I certify that I have read this study and that in my opinion it conforms to acceptable standards of scholarly presentation and is fully adequate, in scope and quality, as a dissertation for the degree of Doctor of Philosophy.

John R. Eyler

John R. Eyler, Chairman
Professor of Chemistry

I certify that I have read this study and that in my opinion it conforms to acceptable standards of scholarly presentation and is fully adequate, in scope and quality, as a dissertation for the degree of Doctor of Philosophy.

Willard W. Harrison
Professor of Chemistry

I certify that I have read this study and that in my opinion it conforms to acceptable standards of scholarly presentation and is fully adequate, in scope and quality, as a dissertation for the degree of Doctor of Philosophy.

D H Powell

David H. Powell
Associate Scientist in Chemistry

I certify that I have read this study and that in my opinion it conforms to acceptable standards of scholarly presentation and is fully adequate, in scope and quality, as a dissertation for the degree of Doctor of Philosophy.

Donn G. Shilling
Professor of Agronomy

I certify that I have read this study and that in my opinion it conforms to acceptable standards of scholarly presentation and is fully adequate, in scope and quality, as a dissertation for the degree of Doctor of Philosophy.

James D Winefordner

James D. Winefordner
Graduate Research Professor of
Chemistry

This dissertation was submitted to the Graduate Faculty of the Department of Chemistry in the College of Liberal Arts and Sciences and the Graduate School and was accepted as partial fulfillment of the requirements for the degree of Doctor of Philosophy.

December 1997

Dean, Graduate School